A comparative study of the thermo-hydraulics of the SNUF test facility core using FLOWNEX and RELAP5

C.S. Zikhali

orcid.org/0000-0002-1436-7319

Mini-dissertation accepted in partial fulfilment of the requirements for the degree *Master of Science in Engineering Sciences with Nuclear Engineering* at the

North-West University

Supervisor: Prof V.V. Naicker
Co-supervisor: Dr J-H. Kruger

Graduation: May 2022
Student number: 24044636

ACKNOWLEDGEMENTS

I would like to thank Professor Vishana Naicker for her support and her wise advice throughout the project. I would also like to thank Dr Jan-Hendrik Kruger for his guidance through the study. Many thanks to the South African Research Chairs Initiative (SARChI) in Nuclear Engineering for the financial assistance, and the NWU for affording me the opportunity to further my studies at the university.

I would like to thank my parents, Amon, and Millicent, for inspiring me to work hard and their continuous support. I would also like to express my thanks to the South African Nuclear Energy Corporation SOC Ltd (NECSA) for the financial support which helped me to complete the degree. Last but not least, I would like to thank the Almighty for giving the strength to never give up.

ABSTRACT

In the current energy mix, South Africa sources its energy from coal power, nuclear power, natural gas, hydro power, and various renewable energy sources. From the Integrated Resource Plan released by the Department of Energy in 2019 (DoE, 2019), it has been envisaged that South Africa aims to pursue an energy mix which is diversified with a reduced reliance on a single or a few primary energy sources. Also, since the current coal fleet is close to the end of its design life together with South Africa's commitment to reduced carbon emissions post 2030, an opportunity was identified for a restructured energy mix. One of the technologies chosen for continued inclusion in this new energy plan was nuclear energy.

With the impending possibility of further nuclear power stations being added to the energy grid in South Africa it is necessary to focus some attention on the extent to which the localisation effort of the country would be carried out in this nuclear build program. Thermo-hydraulic analysis was identified as the area of expertise at the NWU which was to be expanded upon with a specific focus on the modelling of the core region of the Seoul National University Facility (SNUF). SNUF is a small-scale nuclear testing facility located at the Seoul National University and is based on the Advanced Power Reactor 1400 MWe (APR1400) (Lee, 2008).

Simulation tools are used for thermo-hydraulics studies, with the RELAP5 being a popular benchmark simulation package in the nuclear field. Flownex®, which is a locally developed simulation tool in South Africa, is a thermo-hydraulics code which offers a very broad range of options that provide the most relevant solutions to aid in solving various system level and sub-system level simulations (M-Tech, 2013). By further developing this code in the nuclear systems arena, a good foundation could be laid towards the nuclear new build localisation effort. Therefore, the primary objective of this study was to develop a RELAP5 model of the core region and downcomer section of the SNUF facility and then to replicate this model with a corresponding Flownex® model. The ability of both models was then evaluated in predicting the thermo-hydraulic behaviour of the core region of the SNUF facility.

The simulation fidelity of both the RELAP5 and Flownex® models were investigated and compared with each other, specifically the calculation of the heat transfer coefficient and the distribution of the power by the heater elements. The Dittus-Boelter correlation used in

Flownex®, produced unrealistic wall temperatures, while the Chen correlation produced good agreement with the RELAP5 results for the set of conditions used. The fluid bulk temperatures were found to differ by a maximum of 0.03% between RELAP5 and Flownex® but the wall temperatures were found to differ by 359%. It was therefore observed that when Flownex® applied the Dittus-Boelter correlation in its calculations, it produced unrealistic wall temperatures for the set of conditions used. In contrast, when a C# script was embedded within Flownex® using the Chen correlation for its calculations, good results were produced which were in agreement with the RELAP5 results. The conduction analysis study showed that discretisation of the component for both RELAP5 and Flownex® should be properly applied to get consistent results.

Key terms: Thermo-hydraulics, Seoul National University Facility (SNUF), Reactor Excursion and Leak Analysis Program version 5 (RELAP5), Flownex®, Simulation tools.

TABLE OF CONTENTS

LIST OF TABLES

LIST OF FIGURES

List of acronyms

Abbreviation	Meaning
EES	Engineering Equation Solver
IRP	Integrated Resource Plan
KAERI	Korea Atomic Energy Research Institute
MTR	Materials Test Reactor
Nedlac	National Economic Development and Labour Council
NPP	Nuclear Power Plant
PWR	Pressurised Water Reactor
RELAP5	Reactor Excursion and Leak Analysis Program version 5
SNUF	Seoul National University Facility

Nomenclature

Symbol	Description	Unit
A	Area	m^2
A_m	Average area between the surface areas A_1 and A_2	m^2
c_p	Specific heat capacity of the element at constant pressure	$J \cdot K^{-1} \cdot kg^{-1}$
D_{hyd}	Hydraulic diameter	m
H_c	Heat transfer coefficient for forced convection	$W/m^2.K$
H_{FN}	Flownex® heat transfer coefficient	$W/m^2.K$
H_{NB}	Heat transfer coefficient for nucleate boiling	$W/m^2.K$
$P_{wall,sat}$	Saturation pressure at wall	Pa
T_f	Fluid temperature	K
T_{sat}	Saturation temperature	K
T_{wall}	Wall temperature	K
C	Heat capacity	kJ/kg.K
F	Enhanced flow and turbulence	
FA	Flow area	m^2
g	Gravitational constant	$N.m^2.kg^{-2}$
G	Mass flux	$kg/m^2.s$
GC	Geometric circumference	m
h	Height of the annulus	m
h_{fg}	Vapourization enthalpy	J/kg

h_0	Total (or stagnation) enthalpy	J/kg
h_{0i}	Stagnation enthalpy at one inlet	J/kg
h_{0e}	Stagnation enthalpy at one outlet	J/kg
HC	Hydraulic circumference	m
HTA	Heat Transfer Area	m^2
HTC	Heat Transfer Coefficient	$W/m^2.K$
k	Thermal conductivity	W/m.K
k_f	Thermal conductivity of the fluid	W/m.K
L	Length of the heat conduction path	m
$\dot{m}_f$	Mass flow rate of fluid	kg/s
$\dot{m}_e$	Mass flow that exits the control volume	kg/s
$\dot{m}_i$	Mass flow that enters the control volume	kg/s
N	Number of nodes	
Nu	Nusselt number	
P	Pressure	Pa
P_{0e}	Pressure at the outlet of the control volume	Pa
P_{0i}	Pressure at the inlet of the control volume	Pa
ΔP_{0L}	Total pressure loss through the control volume	Pa
Pr	Prandtl number	

$\dot{Q}$	The total rate of heat transferred to the fluid	W/m^2
r	Radius of the element	m
r_1	Inner radii of the annulus	m
r_2	Outer radii of the annulus	m
Re	Reynolds number	
S	Suppression factor	
T	Temperature	K
T_f	Temperature of the fluid	K
T_s	Temperature at the surface of the element	K
T_w	Temperature of the surface of the solid, in this case the surface of the cladding	K
μ	Viscosity	kg/m.s
μ_f	Viscosity of fluid	kg/m.s
μ_g	Viscosity of gas	kg/m.s
q	is the heat rate	W
q''	Heat flux	W/m^2
q'''	The rate at which heat is produced per unit volume	W/m^3
ρ	Density	kg/m^3
ρ_f	Density of fluid	kg/m^3
ρ_g	Density of gas	kg/m^3
$\forall$	Control volume	m^3

$\dot{W}$	The total rate of work done on the fluid	$kg/m^2.s^{-2}$
x	Quality	
z	is the elevation	m
z_i	is the elevation at the inlet	m
δ	Surface tension	N/m
v	Kinematic viscosity of fluid	
α	Thermal diffusivity of fluid	
β	Volumetric thermal expansion coefficient	

CHAPTER 1 INTRODUCTION

Human activity has been drastically increasing the earth's global average temperature by 1 degree Celsius since the pre-industrial period. And if we continue at the current rate, the global temperature rise should reach the 1.5°C threshold between 2030 and 2052 (Innovation, 2019). The impacts associated with a global warming of 1.5°C would be more manageable rather than any other temperatures above the proposed 1.5°C threshold between 2030 and 2052. The combined land and ocean temperature has increased at an average rate of 0.07°C per decade since 1880, however, the average rate of increase since 1981 has been more than twice as great. This additional 0.5°C increase could be avoided by reducing Green House Gas (GHG) emissions in the next 10 years (Innovation, 2019). Climate change is one of the biggest drivers of some countries to source nuclear power to the extent that countries representing over half of the world's population are still committed to building new nuclear power plants (Eberhard, 2011).

The application of nuclear power has become a very important topic in South Africa in recent times since the government is planning on adding additional nuclear power to the electricity grid. The Minister of Mineral Resources and Energy of the Republic of South Africa, Mr Gwede Mantashe, put nuclear energy back into the energy mix considerations in his budget vote speech of 11 July 2019. "The IRP 2019 (DoE, 2019) proposes that the nuclear power program be implemented immediately at an affordable pace and modular scale (as opposed to a fleet approach) and to take into account the technological developments in the nuclear field."

South Africa is also known for its dependence on coal-fired generation which is a large contributor to the country's carbon emissions. It needs an alternate reliable source of power, to reduce its dependence on fossil fuels and decrease its carbon footprint. Hence it has been pursuing other low carbon technologies and this has been reflected in the Integrated Resource Plan (IRP). The IRP incorporates a mix of generation technologies in addition to fossil fuelled generation, which includes cleaner coal, gas, nuclear, renewable and hydrogen fuel cells which also includes battery storage.

For emerging economies such as South Africa, an enticing factor towards nuclear power would be energy availability, allowing the country to have access to an energy source which is available 24 hours a day, 365 days a year and be independent of external factors. An energy infrastructure

is a very important component that sets the tone for economic activity and growth across the country. The energy infrastructure needs to be extensive enough to meet industrial, commercial, and household needs (DoE, 2019). An additional advantage of South Africa, in terms of nuclear power, is the fact that the country has the fourth largest total reserves of uranium worldwide. This could lead to the ability to beneficiate the uranium, enabling the country to produce its own nuclear fuel for its nuclear plants and even carries an export potential to other countries having nuclear power plants. This could ensure a great improvement in energy security.

From the past we have seen how dangerous radioactive releases from nuclear power plant accidents can be. The accidents at Chernobyl, Three Mile Island and the most recent one at Fukushima were examples of how severe and expensive a nuclear accident could be (Ragheb, 2011). As a result of the possible high risks of radiation exposure from nuclear related accidents, safety is a very important factor when it comes to the design and operation of nuclear power plants. As a result of this, safety is made a priority in the design and operation of nuclear reactors.

Economics in nuclear power plant design and operation must also be considered since this will protect the owner's investment by ensuring that the plant works efficiently throughout its lifetime, thus yielding a return on the invested capital. This combination of safety and economics can be achieved by using computational simulations as part of the design process. Computational simulations are mathematical descriptions, or models, of a real system written in the form of computer programs which are subsequently run (Britannica, 2019). The information gained from simulations of nuclear power plants helps to form the basis for the decisions made concerning the design, operation, and overall safety of nuclear power plants.

1.1 Motivation for research

With the possibility of the nuclear new build being carried out in South Africa, it was deemed necessary to focus some attention on the extent to which the localisation of the nuclear build will be implemented. An area of expertise which was chosen as the focal point for this study was the thermo-hydraulic analysis of the core region of a nuclear reactor, which for this study was chosen to be the SNUF test facility. This was done using a locally developed computational tool, Flownex® (M-Tech, 2015), which was used for simulating the thermo-hydraulic behaviour of the SNUF research reactor. Further development of this code could assist with the proposed localisation effort in the nuclear build program. Expertise could be enhanced in the areas of

reactor analysis, specifically the characterisation of the thermo-hydraulic behaviour of the reactor core. Reactor analysis consists of disciplines such as criticality, burnup, shielding, steady state and transient analysis of a reactor. These phenomena must however be studied in the context of the thermo-hydraulic conditions inside the core, to understand the behaviour of a reactor during normal conditions and during postulated accident scenarios. This study was concerned with testing whether the current version of Flownex® was able to accurately model the chosen thermo-hydraulic system or whether further development of the code is required.

To facilitate this, a comparison was carried out between a non-homogeneous, non-equilibrium model using the Reactor Excursion and Leak Analysis Program version 5 (RELAP5) (Information Systems Laboratories, 2001) and a homogeneous equilibrium model using Flownex®. The core of the SNUF test facility was the thermo-hydraulic system chosen, details of which is given later in this chapter. The comparison was carried out by building a model of the core region of the SNUF test facility with both Flownex® and RELAP5 and then comparing these results with each other. After this investigation, an assessment was undertaken to indicate the ability of Flownex® to model a more complex PWR core system. It is also noted that this investigation only applied to the heat transfer coefficient of the fluid and the thermal conductivity of the heat structures of the heated core. To simplify the complexity of the task, a simplified system consisting of the core and the downcomer section surrounding the core was investigated in this study as a starting point for further investigations.

1.2 Seoul National University Facility (SNUF)

To keep up with the stringent safety practices applied in the nuclear industry, extensive thermo-hydraulic experiments and design innovations must be performed for the enhancement of safety standards of operating nuclear power plants. The SNUF test facility is such an experiment. It is a small-scale facility located at the Seoul National University and is based on the Advanced Power Reactor 1400 MWe (APR1400), a nuclear reactor designed by KEPCO/KHNP (KEPCO/KHNP, 2011). In addition, the availability of computational tools such as RELAP5 and Flownex® at the North-West University (NWU) has allowed for the simulation of the core region of the SNUF test facility at the NWU. The boundary conditions used for both models were taken from the MARS input file. The MARS simulation code is a best estimate thermo-hydraulic analysis tool developed by the Korea Atomic Energy Research Institute (KAERI) (Young-Seok Son, 2005).

1.3 Problem statement

With the possibility of a nuclear build program taking place in the near future it would be highly strategic to focus on the extent to which localisation can be implemented into the nuclear build program. An important area of expertise to focus on, would be the thermo-hydraulic numerical simulation of the reactor core. Flownex®, which is a locally developed simulation tool, could be used to carry out these thermo-hydraulic simulations. Further development of this code as applied to nuclear systems could assist with the new build localisation effort. The problem then is to develop numerical models of the SNUF reactor core using the local code Flownex®.

1.4 Aims

The aim of the study was to facilitate a direct comparison between a non-homogeneous, non-equilibrium two-phase model using the RELAP5 simulation code and a homogeneous equilibrium two-phase model using the Flownex® simulation code.

Objectives

The objectives of the study were to understand the nodalisation of the given MARS input file and convert it to a working RELAP5 model. After this working RELAP5 model was shown to be running effectively, a RELAP5 model of the core region and downcomer section of the SNUF facility was developed. This RELAP5 model was reduced to a simpler model of the core region and downcomer section of the SNUF facility. An equivalent Flownex® model was then built. The ability of both models in predicting the thermo-hydraulic behaviour of the SNUF facility was then evaluated.

1.5 Outline of this mini-dissertation

Chapter 2 presents the general theory and the literature survey based on the studies undertaken at the SNUF test facility for the postulated steady state and transient scenarios. It will also include previous thermo-hydraulic studies undertaken at the North West University. This chapter also describes the components of the Advanced Power Reactor 1400 MWe PWR (APR1400) and the Seoul National University Facility (SNUF) and provides supporting information concerning their capability to perform their intended functions.

Chapter 3 presents a detailed explanation of the SNUF facility that was modelled in the study. A detailed description of the model's development of the core region of the SNUF facility in both RELAP5 and Flownex® are also given. This chapter also shows the progression of the models from their simplest form to final completion.

Chapter 4 presents the steady state results of the simulations carried out on both simulation packages. A discussion of the results is also given.

Chapter 5 presents the conclusions reached in the study together with recommendations for further work.

CHAPTER 2 LITERATURE REVIEW AND GENERAL THEORY

2.1 Introduction

This chapter presents a summary of the general theory required for the study and a literature survey based on studies by Yong-Soo Kim (2005) undertaken at the SNUF test facility for postulated steady state and transient scenarios. It will also include thermo-hydraulic studies by Slabbert (2011) and Cilliers (2012) undertaken at the North-West University (NWU) Unit for Energy and Technology Systems. In these NWU studies, research was undertaken on the IAEA benchmark Materials Test Reactor (MTR) which mainly focused on the application of thermo-hydraulic codes on research reactors (Slabbert, 2011). Conducting research on MTRs is very important because it could give insight into complex processes occurring in a power reactor core during operation and postulated accidents.

The computational tools used in these studies provided relevance to the current study as Flownex® and RELAP5 were used to carry out the thermo-hydraulic simulations. The literature study also covered studies carried out at the SNUF facility using the MARS thermo-hydraulic code (Young-Seok Son, 2005) developed by the Korean Atomic Energy Research Institute (KAERI). Various postulated accidents were simulated and assessed at SNUF using the MARS code, which is a thermo-hydraulic code like RELAP5 which was used in the current study. The modelling approach and validation studies carried out in these papers by Slabbert (2011) and Cilliers (2012), helped to assist in creating a clear and concise method for modelling purposes.

2.2 Literature review

The study by Cilliers (2012) was focused on establishing a comparison between a homogeneous two-phase model and a two-fluid two-phase model during operational and safety analysis conditions. The purpose of the study was to determine how the homogeneous two-phase model compared with the two-fluid two-phase model when applied to a U-tube steam generator of a typical Pressurised Water Reactor (PWR). From the literature found by Cilliers (2012) comparing Flownex® to RELAP5, a need was seen to conduct the study and check the behaviour of both these codes in different operational conditions. A steam generator was modelled employing the homogeneous two-phase model and employing the two-fluid two-phase model, RELAP5 being the two-fluid two-phase model and Flownex® the former.

In RELAP5, “two-fluid” refers to two-fluids being modelled e.g., water and a non-condensable gas. In the RELAP5 manual (RELAP5, 2010), “two-phase” is not included in naming the flow, because it is implicitly accepted that water must be modelled in two-phases, since that is one of the main objectives of RELAP5 modelling. In the case of RELAP5, when two-phase flow modelling is being implemented, there are a few models that can be used in addition to the homogenous equilibrium two-phase model as used in Flownex®. These include homogeneous flow, thermal equilibrium, and frictionless flow models. These options can be used independently or in combination. When referring to two-fluid in RELAP5, it is implicit that it is two-phase, since one of the fluids is water.

The geometry of the models was based on technical drawings from the Koeberg Nuclear Power Plant in Cape Town and was simplified to a more usable 1-D fluid model (Cilliers, 2012). For the boiling heat transfer to be modelled accurately with Flownex®, a custom script was written in Flownex® to implement the Chen correlation. This was done because of the calculation of the homogeneous two-phase model not being in agreement with the calculation of the two-fluid two-phase model in the heat transfer region. Large differences were observed between RELAP5, which employed the Chen correlation, and Flownex® which employed the Dittus-Boelter correlation, because of these different heat transfer correlations each software package implemented in the heat transfer region. The power levels that were used to validate these models were set at 60%, 80% and 100%. The results from this study were mainly directed towards the boiler region at the point where the heat transfer from the primary section to the secondary section occurred. It was found that the quality calculated by Flownex® deviated from the quality calculated by RELAP5 by a maximum of 5%. The region closest to the tube sheet showed the largest deviation at the point where the water-level affects the homogeneous solution.

The results showed that the overall heat transfer rate predicted with the RELAP5 two-fluid two-phase model was within 1.5% of the measured data from the Koeberg plant. The results generated by the homogeneous two-phase model for the overall heat transfer were within 4.5% of the measured values. The conclusions of the study suggested that the homogeneous two-phase model is a good alternative simulation tool to the two-fluid two-phase model when it comes to normal operating conditions in a nuclear power plant. Even though some discrepancies were found when comparing the results produced by the two codes in the study, the

homogeneous two-phase model and the two-fluid two-phase model results had excellent agreement under normal operating conditions (Cilliers, 2012).

The purpose of the study by Slabbert (2011) was to gain an understanding of the simulation abilities of the Flownex® simulation package. This was done by undertaking a thermal hydraulics study of a typical pool type research reactor. In this study simulations of the IAEA MTR 10 MW were undertaken for steady state and Loss Of Flow Accident (LOFA) transient conditions. The study aimed to evaluate the Flownex® package by assessing the assumptions and possible shortcomings that were built into the software, defining the most relevant method to model the defined problem, evaluating the compatibility and accuracy of the Flownex® model with regard to the research reactor being modelled and lastly comparing the results found in the study with other previous studies.

The current study aimed to emulate the work of Slabbert (2011) by performing simulations of the thermo-hydraulic behaviour of the Seoul National University Facility (SNUF) which is a scaled down version of the APR1400. In the current study, the Dittus-Boelter correlation in Flownex® produced unrealistic wall temperatures for the set of conditions used, therefore it was necessary to implement the Chen correlation within the Flownex® package to achieve closer results. In the study by Cilliers (2012), a custom script was written for Flownex® to implement the Chen correlation for boiling heat transfer. This was significantly less detailed than RELAP5's solution of a matrix of flow regimes and heat transfer correlations. To model the Chen correlation, an Engineering Equation Solver (EES) (F-chart, 2019) application was embedded within the Flownex® platform. This approach then enabled an extension of the work done by Slabbert (2011).

Simulations by Slabbert (2011) employed the Flownex® simulation package. In order to verify the Flownex® solutions, a model of a single fuel assembly was built in Flownex® then validated with a similar model in EES. After validating the Flownex® model, a model of the reactor core was built, and steady state calculations were carried out for the 10 MW and 12 MW power in order to determine the operating conditions. For the transient simulations, slow and fast Loss Of Flow Accidents (LOFA) were simulated whereby failure of the primary coolant pump was assumed. The results of the different LOFA scenarios were then compared with each other.

For the transient simulations it was shown that the LOFA results for the fuel, cladding, and coolant temperature agreed with the values found in the literature. The temperature predicted by Flownex® was shown to be slightly higher than the temperature given in the literature. No considerable differences in pressure and temperature behaviour were found between the 10 MW and 12 MW reactors except for the fact that the 12 MW reactor had slightly higher temperature trends, corresponding to the higher power level input.

The purpose of the study by Fourie (2011) provided further literature on advanced thermo-hydraulic studies regarding research reactors and conventional pressurised water reactors (PWRs). In this study the simulation of the IAEA 10 MW pool type research reactor was carried out for normal operating conditions and for transient conditions using the RELAP5 MOD4.0 thermo-hydraulic analysis code. To verify the applicability of RELAP5 to this study EES was used in the verification process. This study focused on the Loss Of Flow Accident (LOFA) transient which mainly originates from a primary pump failure which causes a sudden reduction in the flow of the coolant in the primary circuit.

To establish steady state conditions, the core was broken down into its constituent fuel assemblies for modelling purposes. A single fuel assembly was modelled to the effect that the approach, together with its assumptions, was then expanded into the full core. This exact problem setup was duplicated in EES, and the results were compared. The comparison between the RELAP5 and EES results had small differences. These results were caused by the differences in the calculation methodology of the density and viscosity of water between the two codes. It was verified that the total implementation of the RELAP5 code was correct. For the transient simulation, four different postulated accident scenarios were simulated. A slow loss of flow and a fast loss of flow transient were simulated for the 10 MW reactor at steady state power. The final two transients were again slow loss of flow and fast loss of flow transients for the 12 MW reactor at steady state power. The transient results showed similar trends which agreed with results sourced from the literature. The temperatures were slightly higher because of the power profile which was chosen for this study. Similar to the study by Fourie (2011) the core in the current study was also broken down into a simpler form such that models of the heater core of the Seoul National University Facility (SNUF) were built. The aspects of the model that were

studied in detail were the heat transfer coefficient of the fluid and the power distribution applied to the heater elements of the core. Only the SNUF core was studied in this work.

2.3 Reactor systems

This section of the study describes the components of the Advanced Power Reactor 1400 MWe PWR (APR1400) and the Seoul National University Facility (SNUF) and provides supporting information concerning their capability to perform their intended functions. The function of a nuclear power reactor is to generate heat at the rate demanded. In the APR 1400 (PWR), this is done with a reactor core, various internal structures, reactivity control components, and core monitoring instrumentation. The thermo-hydraulic behaviour occurring in the full size APR1400 reactor core can be characterised using the scaled down SNUF.

2.3.1 Advanced Power Reactor 1400 MWe (APR1400)

The Advanced Power Reactor 1400 MWe is a standard evolutionary Advanced Light Water Reactor (ALWR) which has been developed in the Republic of Korea. The APR1400 is a state-of-the-art reactor which utilises the latest technology and incorporates advanced design features to meet the aims of the Korea Nuclear & Hydro Power Company for enhanced economic goals and to address the new licensing safety issues and requirements for improved plant safety (KEPCO/KHNP, 2011). The APR1400 has a primary circuit, consisting of the reactor vessel with two coolant loops. Each coolant loop contains one hot leg, two cold legs, one steam generator, and two reactor coolant pumps (KEPCO/KHNP, 2011). A pressuriser (PZR) is connected to one of the hot legs. The reactor core of the APR1400 consists of 241 fuel assemblies made of fuel rods containing uranium dioxide (UO2). The APR1400 uses slightly enriched uranium, and the reactor core and other related systems are designed to use MOX fuel up to 1/3 of core. A portion of the fuel rods contains uranium fuel mixed with a burnable absorber of gadolinium (Gd2O3) to suppress excess reactivity after fuelling and to help control the power distribution in the core (KEPCO/KHNP, 2011). The uranium dioxide (UO2) fuel in in the form of small cylindrical pellets about 1 cm in diameter and 2 cm long usually concave on the ends. The pellets are then loaded into sealed stainless steel or Zircalloy tubes about 4 m long. The pellets expand axially and fill the void spaces between the pellets when the operating temperature of the fuel is reached (Lamarsh, 1982). The fuel tubes can be known as the cladding. The fuel is cooled by water flowing through the fuel assembly.

The steam generators are located at a higher elevation than the reactor pressure vessel for natural circulation purposes. The two steam generators in the APR1400 and the four reactor coolant pumps are arranged symmetrically (KEPCO/KHNP, 2011). Four Direct Vessel Injection (DVI) lines, included in the reactor pressure vessel design, are connected to the supply core cooling water from the In-Containment Refuelling Water Storage Tank. The APR1400 adopts the DVI method for more effective core penetration of the Emergency Core Cooling (ECC) water. The APR1400 is functional in a variety of operational modes predominantly for the base load full power operation. It can also be useful for a part load operation e.g., load following operation (KEPCO/KHNP, 2011). The APR1400 has various safety systems which include active and passive systems put in place to perform the necessary safety measures (KEPCO/KHNP, 2011). The major safety systems included in the design are the Safety Injection System (SIS), the In-containment Reserve Storage Water Tank (IRSWT), shut down cooling system, safety depressurisation and vent system, auxiliary feedwater system and the containment spray system (KEPCO/KHNP, 2011).

2.3.2 The Seoul National University Facility (SNUF)

The SNUF test facility is a Reduced Height Reduced Pressure (RHRP) integral test loop facility designed to simulate the APR1400 PWR. The geometric configuration of the SNUF is equivalent to the APR1400 which consists of two hot legs and four cold legs (Lee, 2008) as illustrated by the 3D schematic in Figure 2-1. The SNUF consists of 260 heaters put in place to simulate core decay heat. The scaling factors of length and area in the primary system are 1/6.4 and 1/178 with respect to the prototype (Lee, 2008). The SNUF has three intact DVI lines which can supply the Safety Injection (SI) water into the upper downcomer as can be seen in Figure 2-2. The main design parameters for the APR1400 prototype and the SNUF are compared with each other as can be seen in Table 2-1.

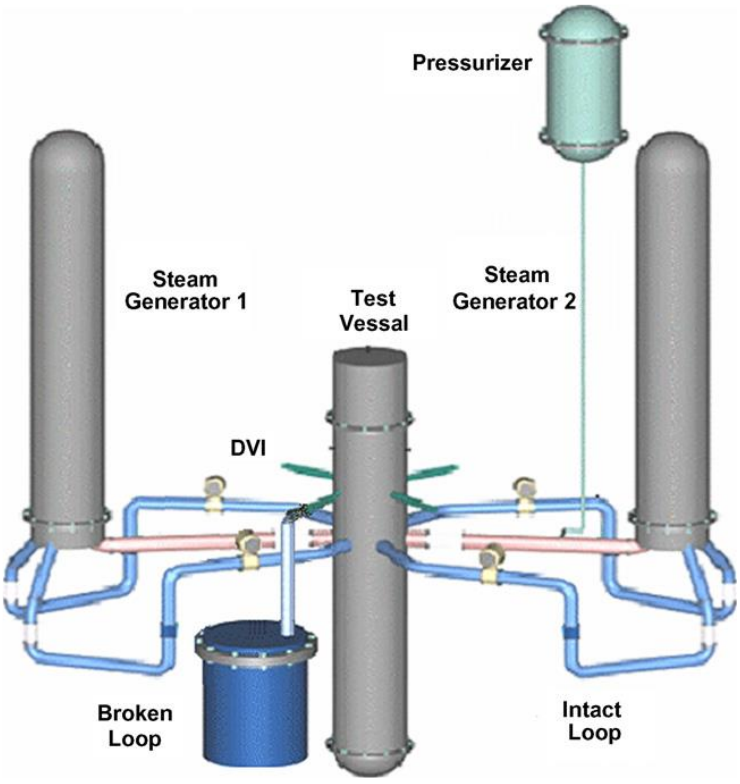

Figure 2-1: 3D schematic of the SNUF (Byoung, 2008).

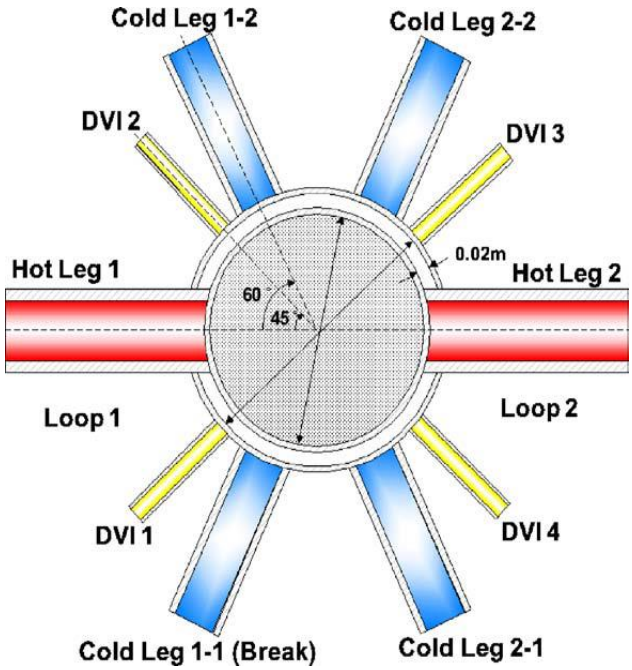

Figure 2-2: Plane view of the SNUF facility (Yong-Soo Kim, 2005).

Table 2-1: Major design parameters.

Parameter	APR1400 Prototype	SNUF
Number of loops	2	2
Volume scale	1	1/1139.2
Area scale	1	1/178
Length scale	1	1/6.4
Core height [m]	3.81	0.6
Primary side volume [m^3]	368.78	0.226
Core volume [m^3]	122.24	0.117
Downcomer volume [m^3]	36.64	0.034
Hot leg volume [m^3]	11.09	0.007
Cold leg volume [m^3]	28.17	0.017
U-tube volume [m^3]	155.58	0.049
Downcomer gap size [m]	0.0255	0.020
Hot leg diameter [m]	1.067	0.064
Cold leg diameter [m]	0.762	0.051

2.3.3 Investigations carried out on the SNUF facility

The main aim of the study by Lee (2008) was to determine the thermo-hydraulic conditions occurring during a Direct Vessel Injection (DVI) line break Loss Of Coolant Accident (LOCA) in the Advanced Power Reactor 1400 MWe (APR1400). In this study the thermo-hydraulic phenomena were analysed at the Seoul National University Facility (SNUF) which, as described earlier, is a scaled down version of the APR1400. This paper was useful for the current study by providing a relevant methodology on how to model the SNUF facility with a thermo-hydraulic simulation package. The boundary conditions for pressure, temperature and mass flow rate were also sourced from this paper. The geometric configuration of the Seoul National University Facility (SNUF) is equivalent to the APR1400 which consists of two hot legs and four cold legs. The SNUF is a type of Reduced Height Reduced Pressure (RHRP) facility. Experimental studies were undertaken at the SNUF to simulate the DVI line break LOCA transient during various conditions. Eight test cases were carried out at the SNUF. The MARS thermal hydraulics code (Lee, 2008) was

used in this study to analyse the transient. To be applicable to conservative conditions it was assumed that the core power was 102% of the normal power and 120% of the decay heat during the transient according to the American Nuclear Society (ANS).

2.3.4 Numerical grid

Independence of the calculation in terms of the numerical grid used is essential, to ascertain the accuracy of the results of a simulation. In order to identify the most suitable mesh which would give an acceptable numerical error, determining grid dependence is important. As the numerical discretisation scheme is improved, the converged solution should become more accurate. This method involves running the simulation on two or more successively finer grids. As the grid is refined the grid cells become smaller and the number of cells in the flow domain are increased. The spatial and temporal discretisation errors should asymptotically approach zero. The easiest approach for generating the series of grids is to generate a grid with what one would consider fine grid spacing, perhaps reaching the upper limit of one's tolerance for generating a grid or waiting for the computation on that grid to converge (NASA, 2008). Variables such as the pressure drop, mass flow, pressure and temperature can be defined as values of interest, since they are the main outputs from the simulation. These values need to converge to asymptotic values otherwise if the simulation runs for additional iterations, the simulation would yield different results. Ensuring that these values have reached an asymptotic solution, means that a decision has been based on a single repeatable value. Before a simulation commences, the values of interest need to be clearly defined and monitored to ensure that an asymptotic solution is met (Leap, 2019).

2.4 General theory

In the analysis of thermal systems, more specifically power conversion systems, the transport equations of mass, momentum, and energy must be considered (Todreas, 1990). The solutions of these transport equations must be suitably prepared for each individual system. In order to prepare these transport equations, general solutions have to be simplified, based on the level of resolution of spatial distributions, the type of fluids involved, and the numerical accuracy required for the analysis (Todreas, 1990).

It has been well documented that conservation equations have different forms between the system codes, but the fundamental equations (conservation of momentum, mass, and energy) are consistent. For each phase in the system, an equation can be written for the conservation of mass, momentum, and energy. During the modelling of hydrodynamic systems, certain challenges come up because of the exchange of mass, momentum, and energy between different phases. The RELAP5 code used in the current study is well suited to modelling two phases, liquid and vapour for the mass, momentum, and energy conservation equations (Glenn, 2014).

2.4.1 Conservation of mass

Mass is a conserved property as it cannot be created or destroyed during a process. The conservation of a mass principle for a control volume can be expressed as: the net mass transfer to or from a control volume during a time interval, Δt is equal to the net change (increase or decrease) in the total mass within the control volume during Δt (Cengel Y., 2008).

This can be expressed as (Incropera, 2002);

$$\cancel{V}\frac{\partial \rho}{\partial t} + \dot{m}_e - \dot{m}_i = 0 \qquad (2\text{-}1)$$

where

$\cancel{V}\frac{\partial \rho}{\partial t}$ is the rate of change of mass within the control volume over time.

2.4.2 Conservation of energy (1st law of thermodynamics)

Energy can neither be created nor destroyed. Energy can only be converted from one form to another. The first law of thermodynamics gives the relation between the three forms of energy namely, heat, work, and internal energy. The convention that is used is that the 'heat' that is added to the control volume is positive. The 'work' done by the control volume on the surroundings is also positive. By stating that energy in the system is conserved it is meant that the energy in the system in the beginning plus the energy transferred to the system must be equal to the energy flowing out of the system plus the energy in the system at the end of the process (Incropera, 2002).

$$\dot{Q} + \dot{W} = \frac{\partial}{\partial t}(\rho h_0 - P) + \dot{m}_e h_{0e} - \dot{m}_e h_{0i} + \dot{m}_e g z_e - \dot{m}_i g z_i \qquad (2\text{-}2)$$

For steady state conditions this becomes:

$$\dot{Q} + \dot{W} = \dot{m}_e h_{0e} - \dot{m}_e h_{0i} + \dot{m}_e g z_e - \dot{m}_\iota g z_i \qquad (2\text{-}3)$$

2.4.3 Conservation of momentum

The conservation of momentum for incompressible flow is given by:

$$\rho L \frac{\partial V}{\partial t} + (P_{0e} - P_{0i}) + \rho g (z_e - z_i) + \Delta P_{0L} = 0 \qquad (2\text{-}4)$$

where

$\rho L \frac{\partial V}{\partial t}$ is the rate of change of momentum per unit length;

$(P_{0e} - P_{0i})$ is the difference in total pressure between the inlet and outlet of the control volume; and

$\rho g (z_e - z_i)$ is the term due to the gravitational force.

2.5 Heat removal from a nuclear reactor

During normal operating conditions when the nuclear reactor is at steady state, all the heat produced in the reactor must be removed as it is produced. This is done by passing a liquid or gaseous coolant through the reactor core. This process of heat removal via a dedicated coolant plays a critical part in the design of nuclear reactors.

Conduction and convection are the most important mechanisms by which heat is removed from a nuclear reactor. Conduction can be defined as the heat transfer in a solid or a stationary fluid (gas or liquid) due to the random motion of its constituent atoms, molecules and/or electrons (Cengel, 2008). The heat produced within the fuel rods is transferred to the surface of the rod through the conduction mechanism. Convection can be described as the transfer of heat between a solid surface and a moving fluid. Convective heat transfer is the transport of heat by the moving fluid. In a moving fluid there can also be conduction by heat transfer, albeit very small compared to other mechanisms. It contributes to the heat transfer between a solid and a liquid (Cengel, 2008). The heat is carried to the surface of the fuel rod through conduction; it is then carried through to the coolant out of the system through convection.

Temperatures in nuclear reactors are usually not the same at various points in the reactor and as a result of this there is usually a single rod in the core which at some point of its length is hotter than all the other rods (Lamarsh, 1982). The power level of the reactor together with the design of the coolant system and the nature of the fuel all contribute significantly to the maximum fuel temperature. Other contributing factors such as metallurgical considerations place an upper limit on the temperature to which a fuel rod can safely be raised (Lamarsh, 1982). The design of the reactor coolant system is carried out in such a way that the heat removed from the reactor at a specific power level ensures that the maximum fuel temperature remains within the predetermined design specifications (Lamarsh, 1982).

2.6 Heat transfer by conduction

2.6.1 Equations governing heat conduction

Fourier's Law forms the fundamental relationship governing heat conduction, which for an isotropic medium, can be written as (Lamarsh, 1982):

$$q'' = -k\vec{\nabla} T \qquad (2\text{-}5)$$

where

q'' is the heat flux, defined such that $\overrightarrow{q''}.\vec{n}$ is equal to the rate of heat flow across a unit area with unit outward normal $\vec{n}$, the units being [W/m^2].

By considering an arbitrary volume dV of a material in a portion of which heat is being produced it can be deduced from the conservation of energy that the net rate at which heat flows across the surface of the volume in steady state conditions, must be equal to the total rate at which heat is being produced within the specified volume. This can be represented in equation form:

$$[Net\ rate\ of\ flow\ of\ heat\ out\ of\ \not{V}] - [rate\ of\ heat\ production\ within\ \not{V}] = 0 \quad (2\text{-}6)$$

The net rate at which heat flows out of the surface of $\not{V}$ is:

$$Heat\ Flow = \int_A \overrightarrow{q''}.\vec{n}\ dA, \quad (2\text{-}7)$$

where the integral has taken over the entire surface.

From the divergence theorem, Eq. (2-7) can also be expressed in the following way,

$$Heat\ Flow = \int_V div\ \overrightarrow{q''}\ dV \quad (2\text{-}8)$$

The total rate of heat production within the volume V is equal to,

$$Heat\ production = \int_V q'''\ dV \quad (2\text{-}9)$$

where, q''' is the rate at which heat is produced per unit volume.

The Eqs. (2-8) and (2-9) can now be substituted into Eq. (2-6). As a result of the integrals being over the same arbitrarily selected volumes, their integrands must be equal, thus yielding the following solution:

$$\nabla q'' - q''' = 0 \tag{2-10}$$

From this, the steady state equation of conduction for heat transfer is derived. By substituting Fourier's law, Eq. (2-5) into Eq. (2-10) and dividing the resulting equation by k, assumed to be constant, the result becomes,

$$\nabla^2 T + \frac{q'''}{k} = 0 \tag{2-11}$$

This equation is also known as Poisson's equation. If we have a region where there are no heat sources, then Eq. (2-11) can be reduced to:

$$\nabla^2 T = 0 \tag{2-12}$$

The equation above is called Laplace's equation.

The differential equations given above can be used to calculate heat transfer in nuclear reactors when heat conduction needs to be considered.

2.6.2 Heat conduction in a plane wall (Cartesian coordinates)

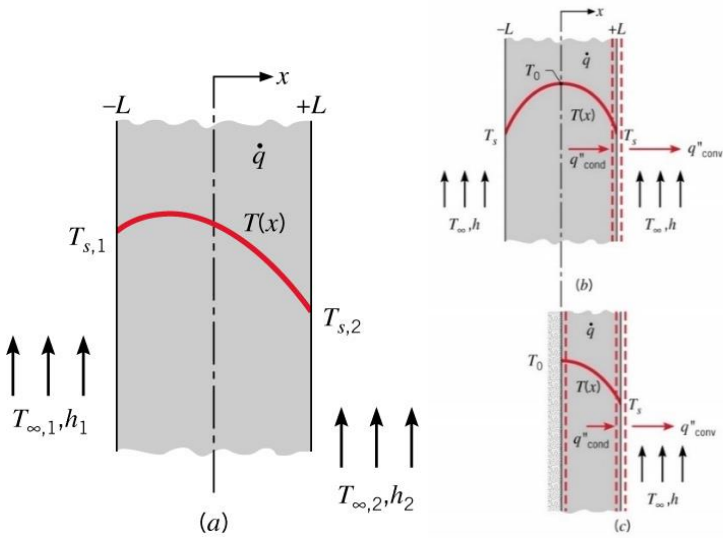

Figure 2-3: Conduction in a plane wall with uniform heat generation. (a) Asymmetrical boundary conditions. (b) Symmetrical boundary conditions. (c) Adiabatic surface at midplane (Incropera, 2002).

Consider a one-dimensional, steady-state conduction in a plane wall of constant *k*, uniform heat generation, and asymmetric surface conditions as shown in Figure 2-3: Conduction in a plane wall with uniform heat generation. (a) Asymmetrical boundary conditions. (b) Symmetrical boundary conditions. (c) Adiabatic surface at midplane. Assume that there is uniform heat generation per unit volume (q''' is constant) and the surfaces are maintained at $T_{S,1}$ and $T_{S,2}$ (Incropera, 2002).

Then Eq. (2-11) becomes,

$$\frac{d^2T}{dx^2} + \frac{q'''}{k} = 0 \tag{2-13}$$

The general solution is,

$$T = -\frac{q'''}{2k}x^2 + C_1\mathrm{x} + C_2 \tag{2-14}$$

where C_1 and C_2 are the constants of integration.

When applying the prescribed boundary conditions,

$$\mathrm{T}(-\mathrm{L}) = T_{S,1} \text{ and } \mathrm{T}(\mathrm{L}) = T_{S,2} \tag{2-15}$$

the constants are:

$$C_1 = \frac{T_{S,2} - T_{S,1}}{2L} \text{ and } C_2 = \frac{q'''}{2k}L^2 + \frac{T_{S,1} + T_{S,2}}{2} \tag{2-16}$$

The temperature distribution then becomes,

$$T(x) = \frac{q'''}{2k}L^2\left(1 - \frac{x^2}{L^2}\right) + \frac{T_{S,2} - T_{S,1}}{2}\frac{x}{L} + \frac{T_{S,1} + T_{S,2}}{2} \tag{2-17}$$

The above result can then be simplified when both the surfaces are maintained at a constant temperature, $T_{S,1} = T_{S,2} = T_s$. As can be seen in Figure 2-3 (b), the temperature distribution then becomes symmetrical about the midplane and is given by:

$$T(x) = \frac{q'''}{2k} L^2 \left(1 - \frac{x^2}{L^2}\right) + T_S \tag{2-18}$$

The maximum temperature exists at the midplane:

$$T(0) = T_0 = \frac{q'''}{2k} L^2 + T_S \tag{2-19}$$

The temperature distribution in Eq. (2-18) can then be written as:

$$\frac{T(x) - T_0}{T_S - T_0} = \left(\frac{x}{L}\right)^2 \tag{2-20}$$

It should be noted that at the plane of symmetry in Figure 2-3 (b), the temperature gradient is zero, $\left(\frac{dT}{dx}\right)_{x=0}$ hence there is no transfer across this plane. This is illustrated as an adiabatic plane in Figure 2-3 (c).

2.6.3 Heat conduction in radial systems (Cylindrical coordinates)

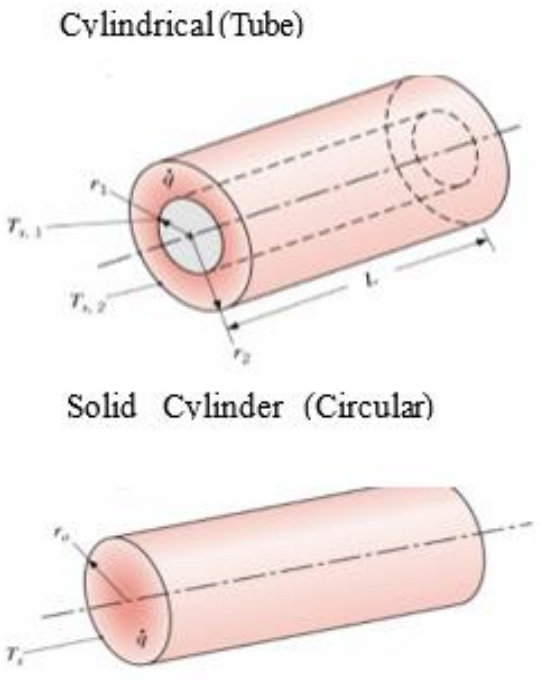

Figure 2-4: Conduction in a solid cylinder with uniform heat generation (Incropera, 2002).

If we consider a heat producing cylinder such as the one in Figure 2-4, then the heat equation can be written in cylindrical co-ordinates as:

$$\frac{1}{r}\frac{\partial}{\partial r}\left(kr\frac{\partial T}{\partial r}\right) + \frac{1}{r^2}\frac{\partial}{\partial \theta}\left(k\frac{\partial T}{\partial \theta}\right) + \frac{\partial}{\partial z}\left(k\frac{\partial T}{\partial z}\right) + q''' = \rho c_p \frac{\partial T}{\partial t} \tag{2-21}$$

where

k is the thermal conductivity and is taken to be constant throughout the volume; and

θ is the tangential coordinate in the cylindrical coordinate system.

In an axisymmetric system there is no change in the tangential direction and the θ dependence can therefore be eliminated from the equation. If we have a constant thermal conductivity k, an infinitely long cylinder, and consider only the steady state, this equation can be reduced to the radial conduction equation,

$$\frac{1}{r}\frac{d}{dr}\left(r\frac{dT}{dr}\right) + \frac{q'''}{k} = 0 \tag{2-22}$$

By using the approximation of an infinite long cylinder, the assumption is being made that axial heat transfer is negligible.

Multiplying by r and integrating we get:

$$r\frac{dT}{dr} = -\frac{q'''}{2k}r^2 + C_1 \tag{2-23}$$

The solution for this equation is:

$$T(r) = -\frac{q'''}{4k}r^2 + C_1 lnr + C_2 \tag{2-24}$$

By applying the boundary conditions,

$$\left.\frac{dT}{dr}\right|_{r=0}$$

and (2-25)

$$T(r_0) = T_s$$

The solution becomes,

$$T(r) = \frac{q'''r_0^2}{4k}\left(1 - \frac{r^2}{r_0^2}\right) + T_s \quad (2\text{-}26)$$

Assuming that the heat source in a cylindrical heater element is evenly distributed throughout the volume, the temperature at the centre of the heater element T_{max} is given by substituting $r = 0$ in Eq. (2-26) to obtain (Bergman, 2011);

$$T_{max} = T_s + \frac{q'''r_0^2}{4k} \quad (2\text{-}27)$$

2.6.4 Flownex® modelling of heat conduction in solids

In Flownex®, a heat source can be implemented in the "distributed heat source" element, spreading the source throughout the element (Leeb, 2016). The heat source can also be applied at a node in a Flownex® model. However, when using the "conduction" element, there is no provision for such modelling, and the heat source must be applied at the conduction element surface, either at the upstream or downstream area of the element.

For heat conduction in a material without an internal heat source, such as the stainless-steel casing of the heater element, two types of heat transfer modelling is possible in Flownex®. One is used for linear one-dimensional heat transfer, and the other is used for cross-conduction heat transfer. Only linear one-dimensional heat transfer was implemented in this study as shown in Figure 2-5. The heat transfer across the element is calculated using the equation:

$$q = kA_m\left(\frac{T_{N1} - T_{N2}}{L}\right) \quad (2\text{-}28)$$

where

q is the total rate heat applied to surface A_1;

T_{N1} and T_{N2} are the temperatures on the corresponding surfaces;

A_m is the average area between the surface areas A_1 and A_2; and

L is the length of the heat conduction path.

The following equation is applicable for cylindrical geometry (Bergman, 2011);

$$q'' = \frac{2\pi hk(T_{N1} - T_{N2})}{\ln\left(\frac{r_2}{r_1}\right)} \tag{2-29}$$

where

T_{N1} and T_{N2} defined above;

r_1 and r_2 are the inner and outer radii of the annulus;

h is the height of the annulus.

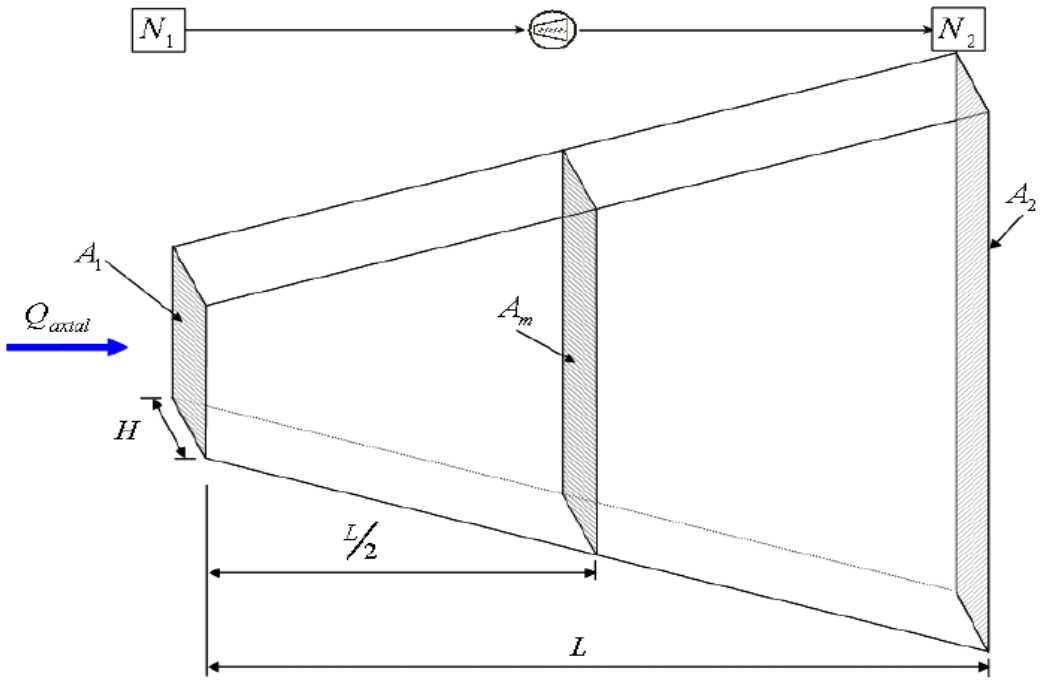

Figure 2-5: Flownex® conduction heat transfer element layout (M-Tech, 2015).

If alternate calculations are required to check the Flownex® and RELAP5 calculations, using for example an Excel calculation, then Eq. (2-28) can be used for slab geometry.

2.7 Heat transfer to coolants

2.7.1 Newton's law of cooling

The heat is generated in the fuel and is then transferred through the gap and the cladding to the surface as discussed in Section 2.3.1. It is then further transferred from the cladding surface to the coolant which transports the heat further into the system. This transfer of heat from the heated source to the fluid is further is discussed in Section 2.7.2. Newton's law of cooling relates the transfer of heat from a heated solid to a moving fluid and is given as (Lamarsh, 1982):

$$q'' = h(T_w - T_f) \tag{2-30}$$

where

h is the heat transfer coefficient [W/m^2-K].

In order to find the total rate of heat across an area *A* between a solid material and a fluid we multiply Eq. (2-30) by *A* to obtain the following equation:

$$q = q''A = hA(T_w - T_f) \tag{2-31}$$

From Eq. (2-31) it is possible to calculate the heat transferred to a coolant for a given difference in temperature between the centre of the fuel and the liquid (Lamarsh, 1982).

2.7.2 Heat transfer in terms of laminar and turbulent flow

One of the most important mechanisms contributing to the effective transfer of heat between a solid surface and a liquid is whether the flow of the liquid in the coolant channel is either laminar or turbulent.

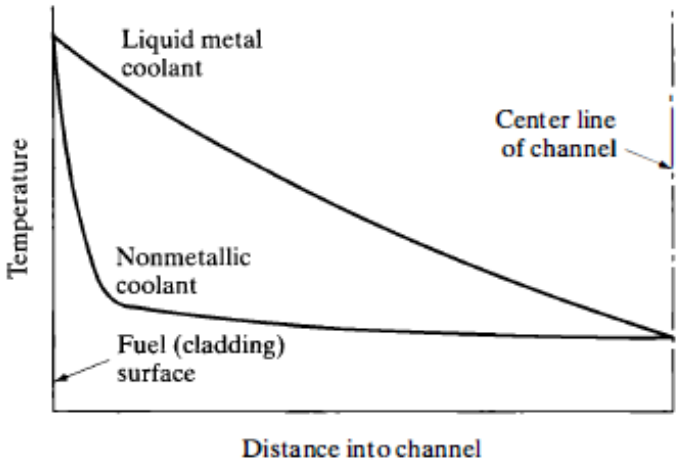

Figure 2-6: Temperature distributions in a non-metallic coolant and in a liquid metal coolant undergoing turbulent flow (Lamarsh, 1982).

In the case where the heat travels radially into the fluid, and where the fluid travels parallel to the wall (laminar flow), the most predominant form of heat transfer will be through conduction. In the other case, where there are radial components of velocity fluctuations occurring within the fluid, some portions of the fluid absorb heat from the wall and transfer it to the centre of the coolant channel, distributing the heat more effectively to the coolant than in the first case mentioned above. The flow in this case would be turbulent.

In cases where the coolant is pumped through the Reactor Coolant System (RCS) as in Pressurised Water Reactors (PWR), the coolant flows under turbulent conditions (Lamarsh, 1982). This turbulent flow results in a more uniform distribution in temperature towards the interior of the coolant channel. As can be seen in Figure 2-6, there is a significant drop in temperature at the wall and it quickly approaches the bulk temperature of the fluid (Lamarsh, 1982). In order to use Eq. (2-31), the heat transfer coefficient h needs to be known. In addition to this, the fluid can experience nucleate boiling. Nucleate boiling is a type of boiling that takes place when the surface temperature is hotter than the saturated fluid temperature by a certain amount but where the heat flux is below the critical heat flux. For water, as shown in Figure 2-7, nucleate boiling occurs when the surface temperature is higher than the saturation temperature by between 10 °C and 30 °C. The critical heat flux is the peak on the curve between nucleate boiling and transition boiling. The heat transfer from surface to liquid is greater than that in film boiling (Lamarsh, 1982).

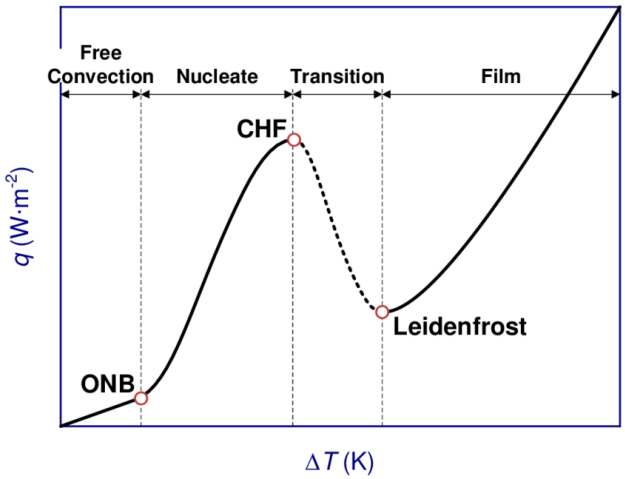

Figure 2-7: Typical boiling curve and regimes (ResearchGate, 2020).

Considering both turbulent flow and nucleate boiling effects, correlations have been developed to calculate the heat transfer coefficient. These would be conditions such as the normal operating conditions in the PWR core whereby fluid flowing up through a fuel assembly is turbulent and experiences nucleate boiling at some axial point of the assembly (Todreas, 1990). One such correlation is discussed in Section 2.7.5.

2.7.3 The Reynolds number

The flow regime of a fluid is characterised using the dimensionless parameter called the Reynolds number which is defined as the ratio between the inertial and viscous forces (Cengel, 2008),

$$\mathrm{Re} = \frac{D_e \mathrm{v} \rho}{\mu} \tag{2-32}$$

where

D_e is the equivalent (hydraulic) diameter [m];

v is the average velocity of fluid [m/s];

ρ is the density of the fluid [kg/m^3];

μ is the viscosity of the fluid [N.s/m^2]; and

D_e can be obtained using the following equation:

$$D_e = 4 \times \frac{Free\ Flow\ Area}{Total\ wetted\ perimeter} \quad (2\text{-}33)$$

2.7.4 Dittus-Boelter correlation

The Dittus-Boelter correlation is a heat transfer expression which can be used for a coolant fluid in a long straight channel (Cengel, 2008). This correlation has been found to be good for conditions where the temperature difference between the channel wall and the bulk fluid is not very large and the Reynolds number is greater than about 10,000. The Prandtl numbers should be between about 0.7 and 120 for this correlation, and the physical properties should be evaluated at the bulk fluid temperature. The Dittus-Boelter correlation defines the Nusselt number as a function of the Reynolds and Prandtl numbers. The Nusselt number Nu is the ratio between the convection and conduction heat transfer and is given by

$$Nu = \frac{hD_e}{k}$$

and the Prandtl number Pr is the ratio of the momentum and thermal diffusivity and is given by

$$Pr = \frac{v}{\alpha} = \frac{C_p \mu}{k}$$

In these equations, the following are defined:

v is the kinematic viscosity of fluid given as $\frac{\mu}{\beta}$;

α is the thermal diffusivity of fluid given as $\frac{k}{\beta C_p}$;

C_p is the specific heat at constant pressure and; and

β is the volumetric thermal expansion coefficient.

Using the above three dimensionless parameters the Dittus-Boelter equation is given as follows (Todreas, 1990):

$$Nu = 0.023Re^{0.8}Pr^{0.4} \tag{2-34}$$

For $0.7 < Pr < 100$ and $Re > 10000$;

All the physical properties are evaluated at the bulk temperature of the fluid (Todreas, 1990).

2.7.5 Chen correlation

The Chen correlation is a widely used heat transfer correlation, that provides for nucleate boiling heat transfer, and is applied in the following manner (Todreas, 1990):

$$q'' = h_c(T_w - T_f) + h_{NB}(T_w - T_{sat}) \tag{2-35}$$

where T_w, T_f and T_{sat} are the wall, bulk fluid and fluid saturation temperatures. The convection coefficient for heat transfer by homogeneous single-phase flow is indicated by h_c and for flow undergoing nucleate boiling conditions it is represented by h_{NB}. These coefficients are calculated as shown in Eqs. (2-36) and (2-37). The convective part, h_c, is a modified Dittus-Boelter correlation given by the equation shown in Eq. (2-36). Chen proposed a correlation where the heat transfer coefficient can be found using the sum of a forced convection (h_c) component and a nucleate boiling (h_{NB}) component. The nucleate pool boiling correlation of Forster and Zuber, shown in Eq. (2-37) is used to calculate the nucleate boiling heat transfer coefficient (h_{NB}) and the modified Dittus-Boelter correlation (h_c) is used to calculate the liquid-phase convective heat transfer coefficient (Todreas, 1990).

$$h_C = 0.023\left(\frac{G(1-x)D_e}{\mu_f}\right)^{0.8}\left(Pr_f\right)^{0.4}\frac{k_f}{D_e}F \tag{2-36}$$

and

$$h_{NB} = 0.00122S\left[\frac{\left(k^{0.79}c_p^{0.45}\rho^{0.49}\right)_f}{\sigma^{0.5}\mu_f^{0.29}h_{fg}^{0.49}\rho_g^{0.24}}\right]\Delta T_{sat}^{0.24}\Delta p^{0.75} \tag{2-37}$$

With

$$S = \frac{1}{1 + 2.53 \times 10^{-6}Re^{1.17}} \tag{2-38}$$

$$Re = Re_l F^{1.25} \tag{2-39}$$

$$\Delta p = p(T_w) - p(T_{sat}) \tag{2-40}$$

$$\Delta T_{sat} = T_w - T_{sat} \tag{2-41}$$

$$F = \begin{cases} 1 & \text{for } \dfrac{1}{X_{tt}} < 0.1 \\ 2.35\left(0.213 + \dfrac{1}{X_{tt}}\right)^{0.736} & \text{for } \dfrac{1}{X_{tt}} > 0.1 \end{cases} \tag{2-42}$$

$$X_{tt} = \left(\frac{1-x}{x}\right)^{0.9}\left(\frac{\rho_g}{\rho_f}\right)^{0.5}\left(\frac{\mu_f}{\mu_g}\right)^{0.1} \tag{2-43}$$

In the above equations, the following definitions apply as stated in Table 2-2:

Table 2-2: Definitions for symbols listed in the Chen correlation (Todreas, 1990)

Parameter	Symbol	Unit
Mass flux	G	kg/m^{2}s
Equivalent diameter	D_e	m
Prandtl number	Pr_f	-
Thermal conductivity	k_f	W/mK
Fluid density in the liquid phase	ρ_f	kg/m^3
Wall temperature	T_W	K
Fluid bulk temperature	T_f	K
Mixture quality	x	-
Fluid dynamic viscosity	μ_f	kg/m. s
Fluid Reynolds number	Re_f	-
Fluid specific heat capacity	$c_{p,f}$	J/kg. K
Fluid density in the vapour phase	ρ_g	kg/m^3
Fluid saturation temperature	T_{sat}	K

The ranges of water conditions for the Chen correlation are as follows (Todreas, 1990):

Pressure: 0.17 – 6.9 MPa

Liquid inlet velocity: 0.06 – 4.5 m/s

Heat flux: up to 2.4 MW/m^2

Quality: 0 – 0.7

The Chen correlation has the benefit of being applicable over the entire boiling region (Todreas, 1990). It also has a lower-deviation error of 11% which is significantly less than the deviations of the correlations by Dengler and Addoms (38%), Bennet et al. (32.6%), and Shrock and Grossman (31.7%) (Todreas, 1990).

In the Flownex® package, the heat transfer coefficient is related to the temperatures T_W and T_f using Eq. (2-30) (M-Tech, 2013))

$$q'' = h_{FN}\left(T_w - T_f\right) \tag{2-44}$$

Here, h_{FN} is the heat transfer coefficient and q'' is the heat flow through the heat transfer area. The Flownex® heat transfer coefficient h_{FN}, can be determined as follows:

- It may be calculated with the aid of a user written script;
- It may be given as a constant by the user; or
- It may be calculated internally by the Flownex® package using the Dittus-Boelter correlation. It is noted that the Gnielinski correlation is also available within the Flownex® package. However, as defined in Vol1, page 568 of Todreas (1990), it is applicable only to single phase heat transfer. Guided by this definition, the results were not expected to differ as significantly from the Dittus-Boelter correlation as with those implementing the Chen correlation. The Gnielinski correlation was therefore not investigated.

The first option given above was used in the current study. By equating Eqs. (2-35) and (2-44) one obtains;

$$h_{FN} = \frac{h_c\left(T_w - T_f\right) + h_{NB}(T_w - T_{sat})}{T_w - T_f} \tag{2-45}$$

In the following chapter, the calculation methodology is described in more detail, and further details are given on how Flownex® calculates the relevant heat transfer coefficient and where it fits into the solution algorithm.

The modelling approach and validation studies carried out in the papers mentioned above assisted in creating a clear and concise method for modelling the core and the downcomer section of the SNUF facility. The thermo-hydraulic behaviour occurring in the full size APR1400 reactor core was characterised successfully using the scaled down SNUF. The RELAP5 code used in the current study was well suited to modelling two-phases, liquid and vapour for the mass, momentum, and energy conservation equations.

CHAPTER 3 METHODOLOGY

3.1 MARS code

The MARS code is a thermo-hydraulic code developed by the Korea Atomic Energy Research Institute (KAERI) based on RELAP5/MOD3.4 and COBRA TF to establish an independent nuclear safety analysis technology capability (Son, 2005). To permit a cost-effective calculation of system transients, the MARS code was developed and was based on a two-phase, non-equilibrium, non-homogeneous hydrodynamic model for the transient simulation of two-phase systems. The two-phase system behaviour is solved by employing a fast, partially implicit numerical scheme (Son, 2005).

3.1.1 Interpreting the MARS input file

The MARS input file was received from the Seoul National University with all the input parameters relating to the SNUF facility. For the input parameters to be correctly defined by RELAP5 and Flownex® the MARS input file was interpreted and all the required input parameters such as the pressures, temperatures, elevation angles, inclination angles, and mass flows were initially transferred to the RELAP5 input file. The geometry and heat structure inputs from the MARS input file are shown in Table 3-1. All the hydrodynamic components were carefully translated from the MARS input file, for the RELAP5 and Flownex® simulations to give the correct results, using their own representative sub models.

Table 3-1: Geometry and heat structure inputs.

		Input Parameters	RELAP5	Flownex®
Pressure	MPa	0.8	0.8	*
T-cold Leg	K	422.74	422.740	*
T-hot Leg	K	434.20	Calculated	Calculated
Power	MW	0.244	0.0488×5	*
$\dot{m}$	kg/s	4.92	4.9182	*

Length of core L	m		0.12×5	0.60
Total Heat Transfer Area 1	m^2	*	*	0.23562
Total Heat Transfer Area 2	m^2	*	*	0.23562
Heat Transfer Area 1/5	m^2	*	0.04712	*
Total Heat Transfer Area 3	m^2	0.23562	0.23562	0.23562
Heat Transfer Thickness 1	m	0.00250	0.00250	0.0025
Heat Transfer Thickness 2	m	0.00250	0.00250	0.0025
Flow Area	m^2	0.04946	*	*
Geometric Diameter	m	0.250947	*	*
Hydraulic Diameter	m	0.02124	*	*
Hydraulic Circumference	M	9.31450	*	*

* The variable was not calculated by the simulation tool in question but was sourced directly from the MARS input file.

3.1.2 Simplification of the geometry

The modelling approach taken to simplify the geometry of the SNUF facility, was to take the full model of the primary side of SNUF and remove all the extraneous components, leaving only the core and the downcomer section around the core. The reason for this was to limit the scope of the current study and that projects following this study could then consider adding the additional components until the entire facility is modelled using Flownex®. The schematic nodalization as modelled in MARS is shown in Figure 3-1, the blue border representing the simplified model, which included the core region. The downcomer section was kept in the model so that the pressure losses could also be accounted for. The simplified nodalization of the core region of the SNUF facility showing the layout of the components together with the numbering of each component, is given in Figure 3-2. However, this illustration excludes the heat structures.

The MARS input model had five axial discretisations for the core, and each axial discretisation was further discretised into six segments to account for the heat flow in the radial and tangential directions. The initial steady state model, referred to as model 1, was represented as a single pipe comprising of five axial discretisations to model the axial and radial heat flow, but the six tangential discretisations were removed. The downcomer was included in the model to account for the heat being transferred from the core, through the downcomer to the surroundings. In this pipe model the flow path was discretized into several discreet elements positioned in series along

the length of the flow path. In the initial RELAP5 steady state model, the downcomer section was represented as five axial sections. The discretisation of the model in RELAP5 is further discussed in Section 3.2.

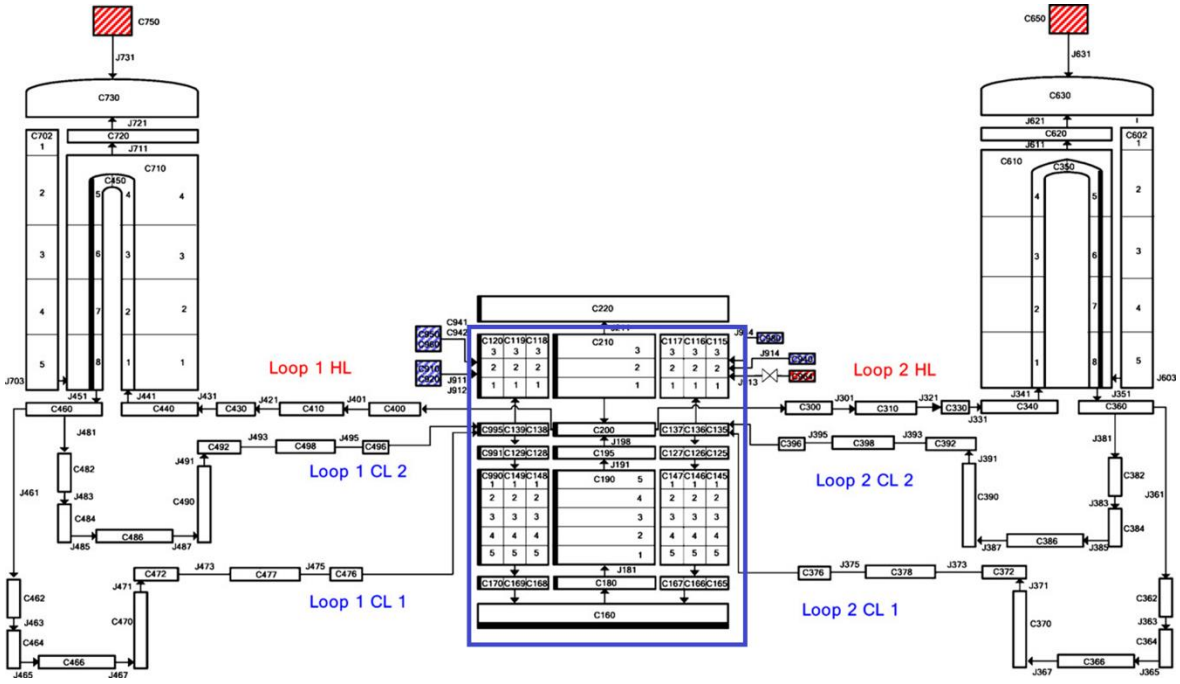

Figure 3-1: RELAP5 schematic nodalisation of the SNUF (adapted from (LEE, 2008)).

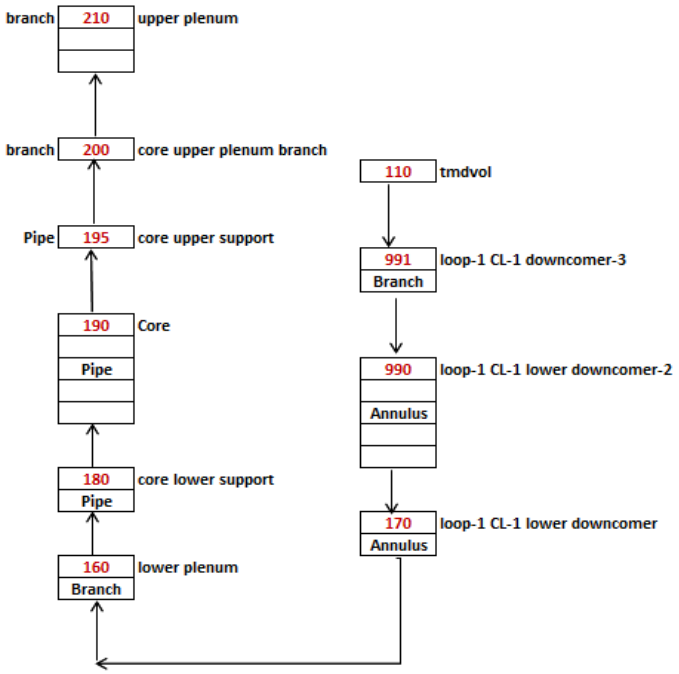

Figure 3-2: RELAP5 nodalisation of the SNUF facility core region.

3.2 RELAP5

The RELAP5 simulation code is used for the purpose of predicting the behaviour of light water reactors during normal and transient conditions. The production versions of this code currently in use are RELAP/SCDAPSIM/MOD3.2 and RELAP/SCDAPSIM/MOD3.4 and are mainly utilised by licensed users and program members for applications such as research reactor and NPP applications (Allison, 2009). The RELAP5 code has been designed to model the coupled behaviour of the reactor core and coolant systems for postulated accidents such as the Loss Of Coolant Accidents (LOCAs) and other operational transients such as the loss of feedwater, loss of flow, loss of offsite power and anticipated transients without scram (RELAP5, 2010).

3.2.1 RELAP5 input structure

The nodalization of a simple pipe on RELAP5 is shown in Figure 3-3. The components can be explained in the following manner.

Wherever flow enters or leaves a hydrodynamic system, hydrodynamic system boundary conditions are defined. A time dependent volume (TMDPVOL) is specifically used where flow enters or leaves a hydrodynamic system and defines the pressure and temperature of the fluid entering or leaving a system. A time dependent junction (TMDPJUN) is used to specify the mass flow rate and must connect a time dependent volume to another hydrodynamic volume in the system. A time dependent junction is always linked to a time dependent volume. Single volumes (SNGLVOL) and pipes (PIPE) are used to define hydrodynamic volumes, and single junctions (SNGLJUN) or multiple junctions (MTPLJUN) are used to connect hydrodynamic volumes. A pipe can be considered as several single volumes connected in series using single junctions. There are several other components that can also be used in RELAP5, such as branches, pumps, trips, etc. These are not discussed here since they were not used in the model, and the reader is referred to appendix B of the RELAP5 input manual (RELAP5, 2010) for further information. Given below in Figure 3-3 is the basic example of a simple pipe taken directly from the RELAP5 input manual, the specifics relating to the models used this study will be given later.

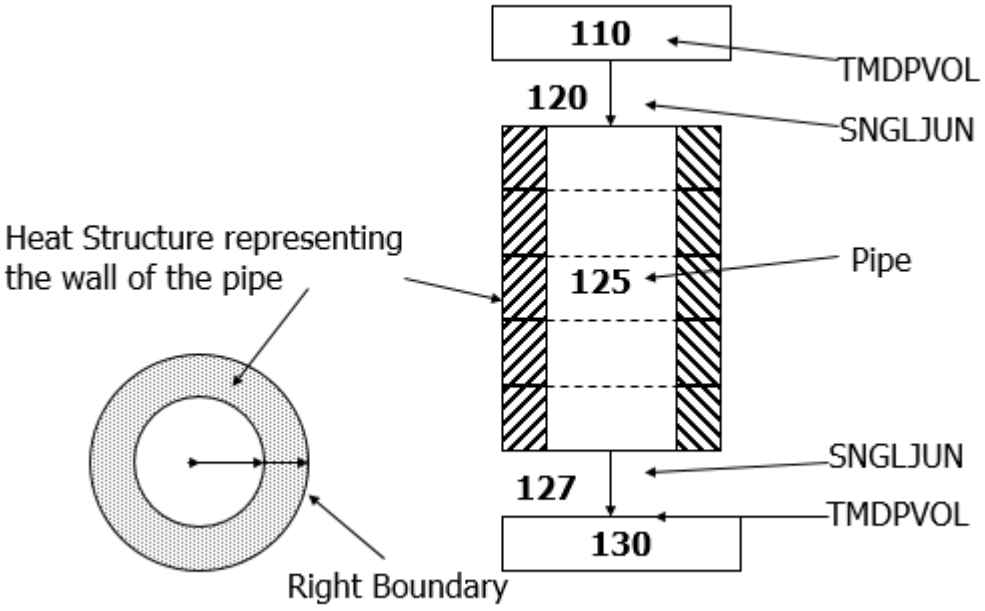

Figure 3-3: Nodalisation of a simple pipe using RELAP5 (Information Systems Laboratories, 2001).

3.3 Flownex®

The Flownex® code uses a homogeneous equilibrium model with the ability to simulate different transients, which can be used to simulate various accident scenarios. Flownex® also allows users to predict, design, and optimise various parameters in fluid systems such as the pressures, temperatures, flow rates, and the heat transfer rates. It offers a relatively fast, reliable, and accurate total system and sub-system approach to the simulation of flow systems (M-Tech, 2013). Flownex® also has the added ability to simulate a variety of systems with any arrangement of liquid, gas, slurry, two-phase, and mixture flows for both steady state and transient conditions (M-Tech, 2013).

The Flownex® simulation code offers a very broad range of options that provide the most relevant solutions to aid in solving various system and sub-system level simulations. This tool also allows the user to carry out various tasks such as the analysis of new concepts while simultaneously adhering to the most stringent quality standards. The code is also well suited for predicting system responses to various operational procedures, control scenarios and accident scenarios by

running accurate transient simulations (M-Tech, 2013). Flownex® applies an implicit pressure correction solution algorithm that results in quick and accurate simulations.

"Flownex® applies an uncoupled solution algorithm in which the different governing equations and supplementary closure equations are solved in sequence. This allows for seamless control of various aspects of the solution process through relaxation parameters, by modifying the number of iterations and the convergence criteria for the solution" (Flownex®, 2019).

The various steps involved in the implicit pressure correction algorithm are shown in the list below in the order in which they are executed.

Implicit Pressure Correction Method – IPCM

1. Guess initial nodal pressures;
2. Calculate mass flows using p-Q relationships;
3. Test continuity of mass flows for all nodes;
4. Adjust pressures to ensure continuity of mass flows for all nodes;
5. Update mass flows using new updated pressures;
6. Repeat 1 to 5 until convergence;
7. Solve the energy equation;
8. Repeat 1 to 7 until convergence; and
9. Move to the next time step and repeat 1 to 8 (Only for transient simulations).

The calculation of the heat transfer coefficient forms an integral part of this study, so from Eq. (2-45) the calculation of the Flownex® heat transfer coefficient is as follows.

Since the standard version of Flownex® does not separately calculate the saturation temperature (T_{sat}), an Engineering Equation Solver (EES) script was imbedded into the Flownex® model to calculate the saturation temperature (T_{sat}) which was then passed to the Flownex® internal calculation process. EES is a general equation-solving program that can numerically solve coupled non-linear algebraic and differential equations. An important capability of EES is the thermodynamic and transport property database of high accuracy that is provided for hundreds of substances in a way that gives it an enhanced equation solving capability (F-chart, 2019).

The linked calculation process had to be done iteratively and was performed in the following manner. A starting value for the Flownex® heat transfer coefficient (h_{FN}) was chosen. Flownex® was then allowed to calculate the wall temperature (T_w), the fluid temperature (T_f) and the pressure of the fluid (P_f). These three values where then passed to the EES script. Using the value of the fluid pressure (P_f), the corresponding value of the saturation temperature (T_{sat}) was obtained from the internal tables of EES. Using Eqs. (2-36) and (2-37), the values of the heat transfer coefficient for forced convection (h_c) and the heat transfer coefficient for nucleate boiling (h_{NB}) were calculated, and finally the Flownex® heat transfer coefficient (h_{FN}) was calculated using Eq. (2-45).

The other parameters that were also calculated in the EES script for use in this formula were

x, ρ_f, ρ_g, μ_f, k_f, which have been defined above in the manuscript. The vapourization enthalpy h_{fg} (J/kg) was also included in the calculations.

The value for h_{FN} was then transferred back to the Flownex® model and the values for T_w, T_f and P_f were calculated. This then became an iterative procedure, and convergence was monitored through the parameter h_c. The initial Flownex® nodalization model of the SNUF facility core is shown below in Figure 3-4. The inputs set for the model are given in Table 3-1. The volumes in the model are made up of pipe volumes and heat structure components. The heat structures represent the selected, solid portions of the thermal-hydrodynamic system. Being solid, there is no flow, but the total system response depends on heat transferred between the structures and the fluid (RELAP5, 2010). Pipe walls can be simulated as heat structures as was the case in this study. Another part of the analysis was performed on the nichrome wire, to which in the context of the SNUF experiments was an electric current which was applied to generate an internal heat source. Since the heat source was applied to the nichrome wire, the stainless steel enclosing this wire acted as a cylindrical conductor between the heat source and the coolant. The stainless steel was therefore considered to be a heat conductor. Further explanation of this analysis is given in Section 4.3. The pipe element was used to calculate the fluid velocity and pressure in a section of the pipe as explained in Section 3.2.1. The conduction element was used for heat conduction calculations in a specific direction. In this pipe model the flow path could be discretised into any number of discrete elements positioned in series along the length of the flow path. The heat transfer element was used for calculating heat transferred through the solid

structures. These heat transfer elements represented the hot nichrome wire which in the context of the SNUF experiments, was an electric current applied producing an internal heat source. This heat was transferred to the fluid in these elements. The cold fluid entered the boundary node at the bottom (shown as Node-0 in Figure 3-4) and the warmer fluid exited at the top node (shown as Node-12 in Figure 3-4). The inlet boundary conditions are given below in Table 3-2.

Table 3-2: Boundary conditions at inlet.

Mass flow rate (kg/s)	Temperature (K)	Pressure (MPA)	Power (W)
4.92	422.740	0.8	48800

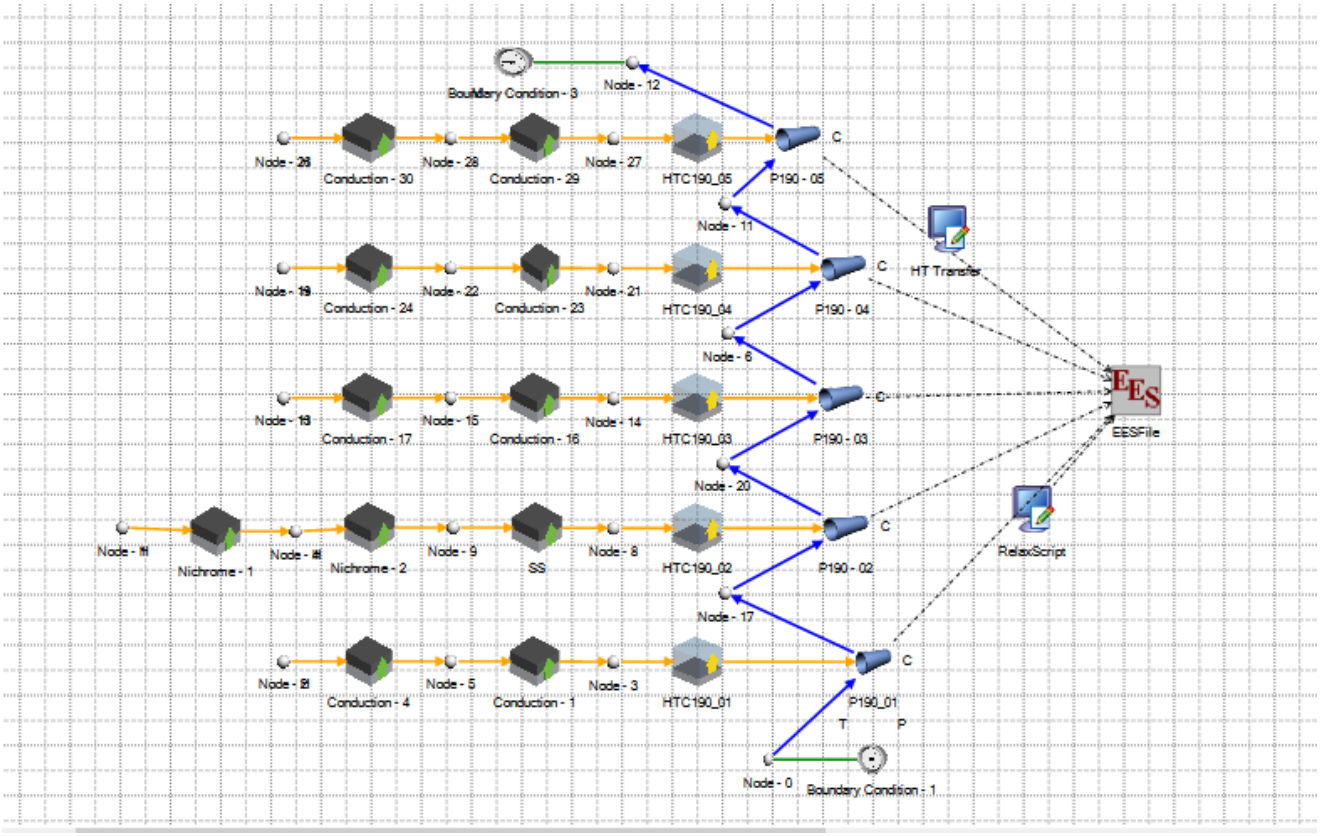

Figure 3-4: Flownex® nodalisation model of the core of the SNUF facility.

The geometry and heat structure inputs used in the Flownex® models were taken from the MARS input file, these inputs are given in Table 3-1. In summary, all the hydrodynamic components were carefully translated from the MARS input file to the RELAP5 and Flownex® models successfully. The modelling approach taken was to simplify the geometry of the SNUF facility, this was done by taking the full model of the primary side of SNUF and removing all the unneeded

components, leaving only the core and the downcomer section around the core. This was done to limit the scope of the study as explained in Section 3.1.2. The ability to predict the thermo-hydraulic behaviour of the SNUF facility by both the RELAP5 and Flownex® models was evaluated successfully. The results from these simulations are shown in the following chapter.

CHAPTER 4 RESULTS AND DISCUSSION

This chapter contains the results and discussions of all the thermo-hydraulic analyses that were performed for this study. In Section 4.1 the focus of the study was mainly on the calculation of the heat transfer coefficient and the wall surface temperatures. The boundary conditions required for this study were the inlet temperature, pressure, mass flow and heat generation inside the nichrome wire, as shown in Table 3-2. The inlet pressure and initial cold leg temperatures were available from the MARS input file as stated in Section 3.1. For this study, a suitable state of the system was required, and the initial boundary values and results found from the analysis of the heat transfer coefficient and wall surface temperature calculations are given in Table 4-4. The nodalization of the given MARS input file was successfully converted to a working RELAP5 model as discussed in Section 3.1. This RELAP5 model was then used as a starting point for all the other RELAP5 models of the core region and downcomer section of the SNUF facility. Equivalent Flownex® models were also built following the RELAP5 models. The ability of both the RELAP5 and the Flownex® models to predict the thermo-hydraulic behaviour of the SNUF facility was then evaluated. The initial RELAP5 results of the base model were evaluated against literature until a sufficient base model was identified. The Flownex® results were evaluated against the RELAP5 results since a sufficient RELAP5 model was identified and also the RELAP5 code can be considered as a benchmark code in the nuclear industry for predicting normal operating and transient conditions in a nuclear reactor. An assumption was made that MARS input model adequately represented the SNUF facility within the constraints and approximations that are normally used when building a system level numerical model.

In the first section of the study the heat transfer coefficient was studied. When fluid flows in the fuel assembly of a nuclear reactor core, specifically a pressurised water reactor (PWR) core during normal operation, it tends to experience nucleate boiling at some axial point of the assembly (Todreas, 1990). Because the rate of heat transfer is much higher under nucleate boiling than for ordinary convective transfer, it is a crucial aspect to address correctly in simulations. Numerous previous studies have investigated the phenomena and correlations that have been developed to calculate the heat transfer coefficient at these conditions. The behaviour of the Dittus-Boelter and Chen correlations was studied under certain thermo-hydraulic conditions. Section 4.2 covered conduction analysis, where discretisation of the heater component for both RELAP5 and

Flownex® was applied to get consistent results. Calculations were performed for conduction with and without internal heat sources. For the calculation without heat sources, the heat source was applied to the nichrome wire and the stainless steel enclosing this wire acted as a cylindrical conductor between the heat source and the coolant. The stainless-steel cladding was therefore considered to be a heat conductor without an internal heat source.

In Section 4.3, distribution of heat sources was studied whereby the conduction was modelled with internal heat sources. The conduction analysis was performed on the nichrome wire where, in the case of the SNUF, an electric current was applied to produce an internal heat source. An assumption was made that the power distribution was both radially and axially uniform. In Section 4.4, axial discretisation of the fluid channel was also studied. In Section 4.5, pressure drop values predicted by RELAP5 and Flownex® are compared and discussed.

4.1 Convection coefficient analysis

The modelling approach was to strip the full model on the primary side of the SNUF facility of all the components, except the core and the downcomer surrounding the core. The downcomer was kept in the model since the heat transfer from the core to the ambient through the downcomer should be considered. In the original model, the downcomer was modelled as five axial sections. Each section was in turn partitioned into six segments so that cross flow in the radial and tangential directions in the plane of the sections could be modelled. It was decided to model the six segments in each section as a single volume, with the result that the downcomer model became five single volumes connected in series, without cross flows. As a result, the only boundary conditions that were required were the mass flow rate, temperature, pressure, and the power which was supplied to the core. The detailed RELAP5 nodalization of the SNUF model which includes the branches and annulus which were excluded in Figure 3-2 for the sake of simplicity, is given in Figure 4-1. Figure 4-1 also accounts for the heat transfer between the core and the downcomer. The components in Figure 4-1 are represented by the following acronyms:

TMDVOL – Time dependant volume

P – Pipe

ANN – Annulus

BR – Branch

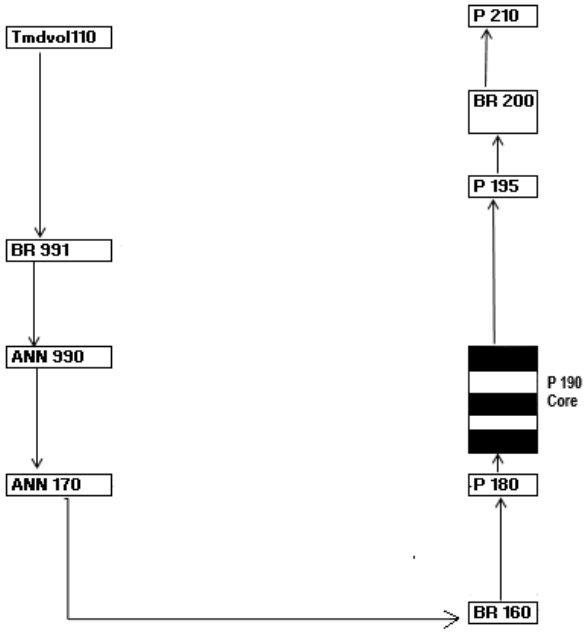

Figure 4-1: Nodalisation of the core region of the SNUF.

The Flownex® model, based on the RELAP5 model shown in Figure 4-1, was built using the specifications from the MARS input. However, the Chen correlation was not available in the Flownex® package as discussed in Section 2.7.5. Therefore, this correlation was modelled using an EES script. However, the heat transfer coefficient, when solved using the Chen correlation, required the wall temperature, which in turn could only be solved with the heat transfer coefficient being known. This therefore required an iterative solution. Since EES normally solved the equations modelled within its framework simultaneously, two C# scripts also had to be used. Flownex® heat structures could only be implemented using the wedge geometry, which used Cartesian coordinates, whereas RELAP5 could use both cylindrical and Cartesian geometry. To verify the results found using RELAP5, similar wedge-shaped models with the same input boundary values were replicated in Flownex®. The base model input parameters are listed in Table 4-4.

The RELAP5 results for the bulk and wall temperature calculations are given in Table 4-1. It was observed that since RELAP5 has the Chen correlation as an inbuilt feature (RELAP5, 2010), there

was an increase in the bulk temperature of the fluid as a result of the fluid being in the sub-cooled state for the entire length of the channel (RELAP5, 2010). The wall temperature remained constant for the length of the entire channel because the fluid at the wall was expected to be at the fluid saturation temperature which caused it to be constant on condition that the pressure drop was small. The increase for the bulk and wall temperatures is shown in Table 4-1. The pipe segments shown in Table 4-1 represent the 5 partitions of the core (P190) as illustrated by the nodalization in Figure 4-1.

Table 4-1: RELAP bulk and wall temperature calculations using the Chen correlation.

Pipe Segments	Units	Bulk Temperatures	Wall Temperatures
1	(K)	423.85	464.17
2	(K)	426.08	464.17
3	(K)	428.34	464.16
4	(K)	430.59	464.16
5	(K)	432.96	464.17

The Flownex® results for the bulk and wall temperature calculations are given in Table 4-2.

Table 4-2: Flownex® bulk and wall temperature calculations using the Dittus-Boelter correlation.

Pipe Segments	Units	Bulk Temperatures	Wall Temperatures
1	(K)	423.89	2066.37
2	(K)	426.19	2096.37
3	(K)	428.49	2129.38
4	(K)	430.78	2163.85
5	(K)	433.07	2200.61

The observation made was, that although the fluid properties from RELAP5 and Flownex® showed some differences, the bulk temperatures were in agreement. As a result of the study

being carried out under steady state conditions, the heat conduction process through the nichrome element allowed for the analysis of this heat conduction to be carried out separately from the convection heat transfer process at the wall-fluid interface. As a verification that this method solved the problem, it was found that the upper and lower temperatures for the bulk fluid temperatures predicted by RELAP5 and Flownex® approach each other.

When using the Dittus-Boelter value for the heat transfer coefficient in Flownex®, a very high value for the temperature, namely 2066.37 K for the 1st pipe increment was observed, as seen in Table 4-2. This value was significantly higher than the value of 464.17 K observed in the RELAP5 results. To investigate this deviation, the RELAP5 value for the heat transfer coefficient was used as temporary input in Flownex® together with the user embedded C# script and the model yielded results which were in much better agreement with the RELAP5 results.

Two sets of results are presented for the Flownex® case in Table 4-3. In the first scenario, Flownex® calculated the Heat Transfer Coefficient (HTC) using the Dittus-Boelter correlation and in the second scenario it used the Chen correlation. In the first scenario where the Dittus-Boelter correlation was used, it can be observed that the wall temperature increases over the length of the heated channel, because nucleate boiling was neglected. The values being calculated for the heat transfer coefficient (h) were low, which indicated that h was being under-estimated. There is thus an inconsistency between the RELAP5 and the Flownex® wall temperature results, as shown in Table 4-1 and Table 4-2.

When the Chen correlation was then used to calculate the heat transfer coefficient, the wall temperatures generated by Flownex® showed agreement with those found with RELAP5. The wall temperatures were showing differences of less than 1 K as can be seen in Table 4-1 and Table 4-2. The heat transfer coefficient values calculated, using the Chen correlation in Flownex®, are shown in Table 4-3. They are in good agreement with the values calculated by RELAP5, approaching convergence at pipe segment 5 as seen below. The difference between the RELAP5 and the Flownex® values are shown in Table 4-3, with the smallest difference at the last pipe segment. A key influencing factor to be noted is that the pressure used during this study falls outside the range of the Chen correlation. To account for this, it is recommended that the calculated temperatures found in this study should be compared to experimental values to

validate the Chen correlation within this range. These experimental values were unfortunately unavailable for this validation process.

Table 4-3: Calculation of the heat transfer coefficient in the five pipe segments.

Pipe Segments	Units	Flownex® Dittus-Boelter	Flownex® Nucleate Boiling	HTC (RELAP5)	[1]HTC (Flownex®)	RELAP5 - Flownex®
1	($W/m^2.K$)	1425	44863	48250	46288	1962
2	($W/m^2.K$)	1429	45419	48319	46848	1471
3	($W/m^2.K$)	1434	45979	48455	47413	1042
4	($W/m^2.K$)	1437	46543	48585	47980	605
5	($W/m^2.K$)	1441	47112	48715	48553	162

A discussion on the implementation of the Chen correlation is now presented. To model the Chen correlation effectively within Flownex®, an EES application was inserted within the Flownex® platform. The properties of the fluid were sourced from the EES and the Flownex® data banks, according to the boundary values applied at the time. The Chen correlation requires both the wall temperature and the heat transfer coefficient for its calculation purpose; hence an iterative process was adopted as is described next. Two C# scripts were written by a member of the DST/NRF SARChI Chair in Nuclear Engineering at the NWU and then embedded within the Flownex® platform to account for this iterative process. The 1st script transferred the wall temperature calculated at each node from the Flownex® calculation to the EES calculation, and then the 2nd script transferred the calculated heat transfer coefficient from the EES calculation back to the Flownex® calculation. The heat transfer coefficient was treated as constant during the iteration process within the Flownex® platform. This process is illustrated in Figure 4-2.

[1] Calculated using a user written script

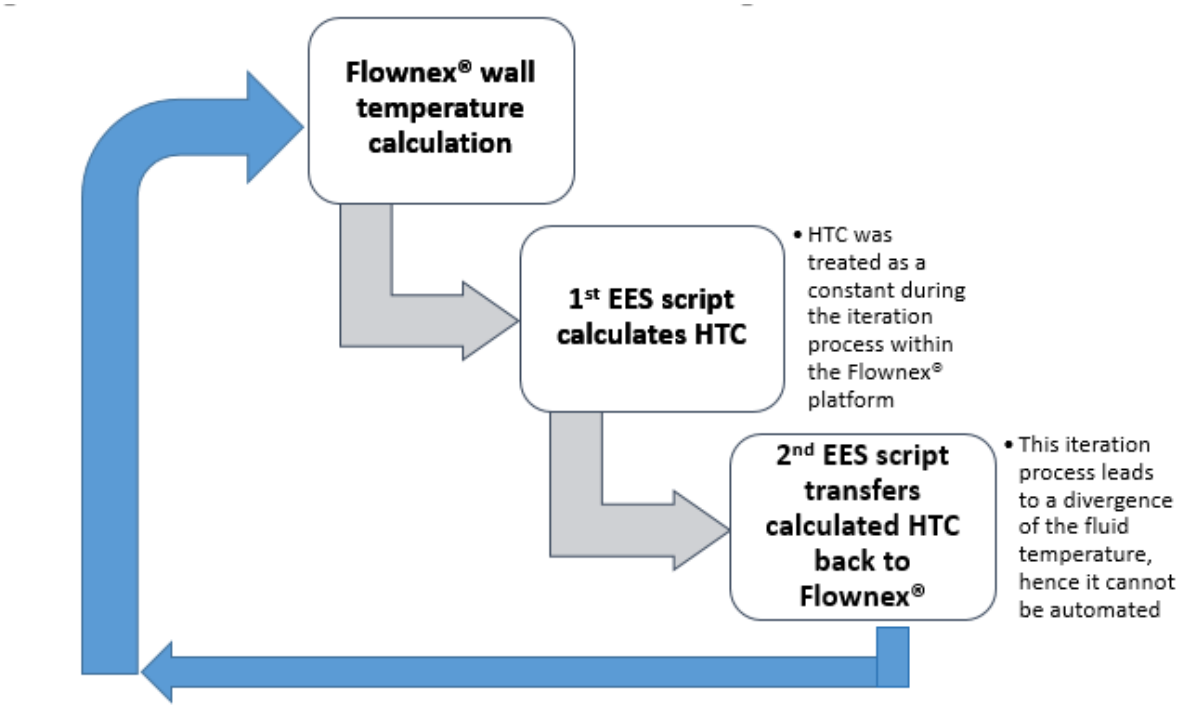

Figure 4-2: Flow diagram showing calculation of heat transfer coefficient using EES script.

This iteration process led to a divergence of the fluid temperature. As a solution to this problem, limits were placed on the wall temperature to control this numerical behaviour. To further explain this process, for a given mass flow rate, pressure, temperature, and power, the wall temperature and the heat transfer coefficient were set to correspond to a specific pair of values which were called the limiting values T_o and h_o. This limit-based approach commenced with two initial guesses for the wall temperatures, T_L and T_U, which were on either side of the expected value. The heat transfer coefficient was calculated for both these temperatures and then the wall temperatures were T'_L and T'_U were subsequently calculated. The temperatures obtained can then be used as the starting values for the next set.

These starting values, T_L and T_U, can be used to calculate the wall temperatures T'_L and T'_U. By continuing with this method of the iterative scheme, the difference between T'_L and T'_U can be calculated until the required precision is found. This will occur when T_L and T_U converge to the same value. As an illustration of the iteration process, a few iteration pairs for (T_L, T'_L) and (T_U, T'_U) are shown in Figure 4-3.

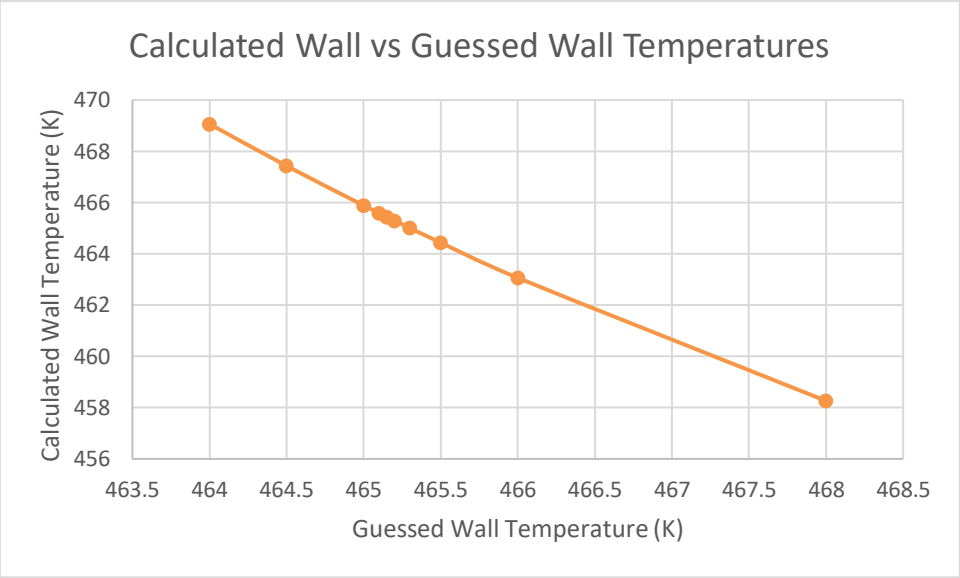

Figure 4-3: Calculated wall temperature vs. the guessed wall temperature.

As this is a user intervention method applied manually in the control loop between the two software codes, it is not yet possible to automate the process for transient calculations. To illustrate numerical convergence for the coupling technique, it was confirmed that the upper and lower temperatures approached each other as shown in Figure 4-3. The numerical divergence (using unbounded values) that was observed, could be due to several reasons e.g., the numerical implementation in the Flownex® code. This problem could form the basis for future studies.

The Chen correlation is a popular correlation when modelling the heat transfer to a fluid when the fluid is in two-phases as stated in Section 2.7.5. This includes the regime of nucleate boiling. The correlation is given as the sum of two terms, the modified Dittus-Boelter correlation given by Eq. (2-36) and the nucleation part given by Eq. (2-37). The thermo-hydraulic parameters calculated during the modified Dittus-Boelter calculation include the following parameters:

- the Heat Transfer Area (HTA) of the pipe representing the core;
- the Flow Area (FA) across the core;
- the circumference and hydraulic diameter of the pipe simulating the core;
- the fluid and saturation temperatures of the coolant in the core; and
- the viscosity, surface tension, heat capacity, thermal conductivity, density, and quality of the fluid.

The results for the analysis of the convection coefficient are presented in Table 4-4. For this state the pressures between RELAP5 and Flownex® calculation differed by a margin of 1000 Pa. This difference was a result of the time dependent volume of RELAP5 applying a larger pressure drop than the Flownex® model of pipe 110. The time dependant volume of the RELAP5 model and pipe 110 of the Flownex® model simulating the same conditions. The pressure drops are discussed in more detail in Section 4.5. The core power between the two packages, represented as the equivalent heat flux, was also in agreement but only had a small marginal difference of 0.21 W/m^2. By using the inlet cold leg temperature, the RELAP5 and the Flownex® calculations were performed and the mass flow rate was adjusted to give the required hot leg temperature. This was adjusted to match the hot leg temperature as given in the study by Byoung (2008).

The value of the mass flow rate was found to be 4.92 kg/s. This value was significantly larger than the value of 0.083 kg/s given by Byoung (2008). As the RELAP5 calculations were performed, the mass flow rate was adjusted to yield the required hot leg temperature according to the input parameters given in Table 3-1 hence giving a mass flow rate different from the one given by Byoung (2008). This larger mass flow rate had an impact on the convective heat transfer coefficient, giving a significantly larger HTC as compared to the one found in literature. The adjusted mass flow rate also had an impact on the calculated pressure drops which is shown later in Section 4.5. The viscosity between the two packages was also very close with a 0.000002 kg/m.s difference between the RELAP5 and the Flownex® values. The density values between the two packages were also very close with a 0.11 kg/m^3 difference between the RELAP5 and the Flownex® values. The quality values for RELAP5 and Flownex® were found to be 0.00008 and -0.039233 respectively, both indicating that the coolant mixture was in fact a saturated liquid. The negative value for the quality given by Flownex® serves to indicate that the fluid is fully saturated e.g., only liquid water is present (Flownex®, 2020). The value for the viscosity given by Flownex® was 0.000179 kg/m.s. The RELAP5 values for the viscosity of the gas and liquid could not be extracted from the RELAP5 output files. “This is because the transport properties phasic viscosities μ_g, μ_f, phasic thermal conductivities k_g, k_f, and surface tension σ are evaluated as functions of the local thermodynamic properties. Also, correlations from the American Society of Mechanical Engineers (ASME, 1967) and Schmidt (Schmidt, 1969) are used for steam and liquid water. The presence of non-condensables in the vapour phase is accounted for by using Wilke’s semi-empirical formula (Wilke, 1950) for μ_g, and by using Mason and Saxena’s analogous method

(Mason, 1958) (with approved modification by Bird, Stewart, and Lightfoot (Bird, 1960) for k_g" (RELAP5, 2010).

Table 4-4: Heat transfer coefficient and wall surface temperature calculations.

Parameter	Symbols	Units	RELAP5	Flownex®	EES	EES Calculation
Power	Q	[W]	48800	48800		
Heat Transfer Area	HTA	[m^2]	0.04712	0.04712		
Power	Q	[W/m^2]	1018591.63	1018591.42		
Flow Area	FA	[m^2]	0.04946	0.04946	0.04946	
Circumference	C	[m]		9.3145	9.3145	
Pressure	P	[Pa]	798940.00	799990.00	799990.00	
Fluid Temperature	T_f	[K]	426.1	426.2	426.2	
Saturation Temperature	T_{sat}	[K]	443.5	443.6		443.6
Wall Temperature	T_{wall}	[K]	464.2	465.2	465.2	
Viscosity	μ	[kg/m.s]	0.000177	0.000179		0.000179
Heat Capacity	C	[kj/kg.k]	4318.68	4314.33		4319.00
Thermal Conductivity	k_f	[W/m.K]	0.684	0.682		0.668
Surface Tension	**σ**	[N/m]	0.04438	0.04809		0.04809
Viscosity of Fluid for Chen correlation in Flownex®	u_f	[$N.s/m^2$]		0.000179		0.000179
Viscosity of gas for Chen	u_g	[$N.s/m^2$]		0.000015		0.000015

correlation in Flownex®						
	h_{fg}	[J/K]	1930992	2.05E+06		2.05E+06
Hydraulic Diameter	D_{hyd}		0.02124	0.02124		0.02124
Density of Fluid	ρ_f	[kg/m^3]	914.20	914.31		914.40
Density of Gas	ρ_g	[kg/m^3]	4.16	4.16		4.16
Quality	x		0.00008	-0.039233		-0.03197
Mass Flow Rate of Fluid	$\dot{m}_f$	[kg/s]	4.92	4.92		
Reynolds Number	R_e		11904.00	11827.40		12259.00
Heat Transfer Coefficient	HTC	[W/m^2.K]	48319.00	26586.95		26587.0
Heat Transfer Coefficient for Forced Convection	H_c	[W/m^2.K]		1216.62		1429
Heat Transfer Coefficient for Nucleate Boiling	H_{NB}	[W/m^2.K]		45419		45419
Flownex® Heat Transfer Coefficient	H_{FN}	[W/m^2.K]		26587		26587
Saturation pressure at wall	$P_{wall,sat}$	[Pa]				1312000
Mass flux	G	[kg/m^2 .s]		99.47	99.47	

Prandtl number	Pr			1.13		1.16
Enhanced flow and turbulence	F			1		1

To further verify the Flownex® results, the results required for the calculation of the heat transfer coefficient for forced convection using the modified Dittus-Boelter correlation are shown in Table 4-5, where it can be seen that they are in good agreement with a 19.78 W/m^2.K difference. The change in saturation temperature was also close, with a 0.05 K difference. The wall pressure between RELAP5 and Flownex® was in agreement. The wall temperature of 464.36 K calculated using the Chen correlation, shown in Table 4-6, was found to be in agreement with the RELAP5 wall temperature of 464.17 K as shown in Table 4-1. Since the Chen correlation produced good agreement with the RELAP5 results, it is suggested that the Chen correlation be implemented in Flownex®, rather than using a user coded script for boiling applications.

Table 4-5: Calculation of the heat transfer coefficient using the modified Dittus-Boelter correlation (Todreas N.E., 1990).

Parameter	Symbols	Units	Flownex®
	A1		12291.42
	A2		1869.31
	A3		33.71
Heat Transfer Coefficient for Forced Convection	h_c	[W/m^2.K]	1449.31
	Calculation of h_{nb}		
Change in Saturation Temperature	ΔT_{sat}	[K]	21.55
Wall Pressure	P_w	[Pa]	1312000

Table 4-6: Calculation of the wall temperature.

Parameter	Symbols	Units	Flownex®
Change in Saturation Pressure	ΔP_{sat}		512010
Suppression Factor	S		0.87
	B1		901.941
	B2		0.827
Heat Transfer Coefficient for Nucleate Boiling	h_{nb}	[W/m^2.K]	46391.23
Wall Temperature	T_w calculated again	[K]	464.36

There was a good correspondence between RELAP5 and Flownex® in the nucleate boing region but not in the single-phase liquid region. A possible reason for this discrepancy could be within the implementation of the Dittus-Boelter correlation, so it is recommended that a laminar correlation be included in the C# script and a turbulent correlation be included in the Dittus-Boelter correlation for single-phase liquid and then tested in Flownex®.

4.2 Conduction analysis at heat structures

Another part of the study was focused on the heat structures. With the heat source applied to the nichrome wire, the stainless steel enclosing this wire acted as a cylindrical conductor between the heat source and the coolant. The stainless steel was therefore considered to be a heat conductor without an internal heat source. Although this is a cylindrical system, slab models for both RELAP5 and Flownex® were first developed. This is because the heat structures in Flownex® could only be modelled, using wedge geometry which can be equivalent to cylindrical coordinates whereas RELAP5 could use both cylindrical and Cartesian geometries. From Table 4-7 the temperature at the interface between the nichrome heater and the stainless-steel

cladding had good agreement between the Flownex® and the RELAP5 calculations. The difference of about 1 K was due to the bias at the wall temperature.

Table 4-7: Fuel centreline and heater element temperature results.

	SS/Nichrome Interface Temperature		Fuel Centerline Temperature	
	RELAP5 (K)	Flownex®(K)	RELAP5 (K)	Flownex® (K)
1	602.04	603.33	707.10	803.48
2	602.04	602.93	707.09	803.15
3	602.04	602.59	707.09	802.87
4	602.04	602.31	707.09	802.64

The difference between the Flownex® and the RELAP5 interface temperatures for the stainless-steel slab were calculated to be about 1 K for all axial discretisations for both codes. Furthermore, a calculation using Eq. (2-28), which was applicable for a steady state calculation, also yielded a value which was slightly higher. The RELAP5 and Flownex® fuel centerline temperatures shown in Table 4-7 had marked differences between them. For the first increment RELAP5 had a fuel centerline temperature of 707.10 K while Flownex® had a temperature of 803.48 K showing a difference of 96.38 K. These fuel centerline temperatures did however approach each other towards the fourth increment. The RELAP5 temperature was 707.09 K while the Flownex® temperature was 802.64 K with a difference of 95.55 K. In these calculations, the conductivity of the stainless steel was taken to be a constant. The slab model results showed good agreement between the RELAP5, the Flownex® and the Excel calculations using Eq. (2-28), as can be seen in Table 4-8. The results for this model are illustrated in Figure 4-4.

Table 4-8: Slab geometry: 1 radial discretisation.

	T_{wall} (K)	T_{wall} (K)	$T_{interface}$ (K)	$T_{interface}$ (K)	$T_{interface}$ (K)	ΔT (K)
	Flownex®	**RELAP5**	**Flownex®**	**RELAP5**	**Calculation Eq. (2-28)**	**Flownex®-Calculation**
Increment 1	465.24	464.17	603.00	602.04	603.00	0.00
Increment 2	465.15	464.17	602.93	602.04	602.90	0.03
Increment 3	465.07	464.16	602.85	602.04	602.90	-0.05
Increment 4	465.05	464.16	602.83	602.04	602.80	0.03
Increment 5	465.02	464.17	602.81	602.04	602.80	0.01

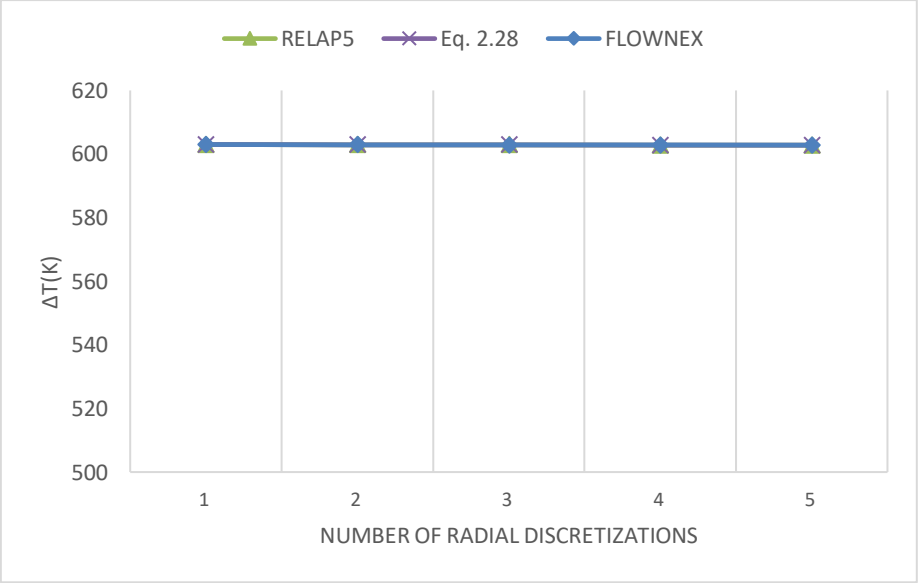

Figure 4-4: ΔT as a function of 1 radial discretisation for the slab geometry.

The cylindrical models required more than one discretisation to achieve more consistent results, so models were built with 1, 2, 4 and 8 discretisations in the radial direction. Unlike the cylindrical models, the slab model only required 1 radial discretisation to give convergent results between the RELAP5, the Flownex® and the Excel calculations. For the cylindrical models, the stainless steel was modelled as a single annulus, with inner and outer radii 0.0025 m and 0.0050 m respectively. The RELAP5 and the Flownex® results were compared to the calculations using Excel, given by Eq. (2-29). The difference between the Flownex® and the RELAP5 wall and

interface temperatures for the cylindrical model with one radial discretisation were calculated to be about 1 K for all axial discretisations for both codes. The difference between the RELAP5 and the Excel calculation of the interface temperatures was also calculated to be about 8 K for all axial discretisations as can be seen in Table 4-9 to Table 4-12. It was found that the temperature difference between the Flownex® and the RELAP5 results at the interface was about 1 K as can be seen in Table 4 15. From Table 4-9 the RELAP5 and the Flownex® temperature results at the interface are in agreement even though Flownex® uses the wedge geometry to calculate its results and RELAP5 doesn't use this wedge geometry. "One-dimensional heat conduction in rectangular, cylindrical, and spherical geometry can be used to represent the heat structures in any of the components in RELAP5. It is assumed in one-dimensional heat conduction that the temperature distribution in the axial or radial direction is the same throughout the structure being modelled and that the linear heat flow is negligible" (RELAP5, 2010).

The temperature difference between the Flownex® and the Excel calculations had a maximum of about -7 K across all axial discretisations. The slab models showed good agreement between the RELAP5, the Flownex®and the calculations in Excel using Eq. (2-28). The cylindrical models required discretisations of 4 or more, compared to the Excel calculations based on Eq. (2-29). These observations were made for both the RELAP5 and the Flownex® models. Another observation made based on the results from Table 4-9 to Table 4-12 was that the results produced by Eq. (2-29) are independent of the number of increments/discretisations because it is a proper cylindrical formulation, and that the RELAP5 and Flownex® (wedge based) results progressively converge to the cylindrical results as the number of discretisations / increments increase.

Table 4-9: Cylindrical geometry: 1 radial discretisation.

Pipe Segment	T_{wall} (K)	T_{wall} (K)	$T_{interface}$ (K)	$T_{interface}$ (K)	$T_{interface}$ (K)	ΔT (K)
	Flownex®	RELAP5	Flownex®	RELAP5	Calculation Eq. (2-29)	Flownex®-Calculation
1	465.24	464.17	646.03	645.09	653.20	-7.16
2	465.15	464.17	645.95	645.09	653.20	-7.24
3	465.07	464.16	645.89	645.09	653.10	-7.21

4	465.05	464.16	645.87	645.09	653.10	-7.23
5	465.02	464.21	645.85	645.09	653.00	-7.15

Table 4-10: Cylindrical geometry: 2 radial discretisations.

Pipe Segment	T_{wall} (K)	T_{wall} (K)	$T_{interface}$ (K)	$T_{interface}$ (K)	$T_{interface}$ (K)	ΔT (K)
	Flownex®	RELAP5	Flownex®	RELAP5	Calculation Eq. (2-29)	Flownex®-Calculation
1	465.241	464.168	650.88	649.93	653.20	-2.32
2	465.153	464.166	650.80	649.93	653.20	-2.40
3	465.075	464.165	650.73	649.93	653.10	-2.37
4	465.052	464.164	650.71	649.93	653.10	-2.39
5	465.029	464.168	650.69	649.93	653.00	-2.31

Table 4-11: Cylindrical geometry: 4 radial discretisations.

Pipe Segment	T_{wall} (K)	T_{wall} (K)	$T_{interface}$ (K)	$T_{interface}$ (K)	$T_{interface}$ (K)	ΔT (K)
	Flownex®	RELAP5	Flownex®	RELAP5	Calculation Eq. (2-29)	Flownex®-Calculation
1	465.241	464.168	652.28	651.33	653.20	-0.92
2	465.153	464.166	652.20	651.33	653.20	-1.00
3	465.075	464.165	652.13	651.32	653.10	-0.97
4	465.052	464.164	652.11	651.32	653.10	-0.99
5	465.029	464.168	652.09	651.33	653.00	-0.91

Table 4-12: Cylindrical geometry: 8 radial discretisations.

Pipe Segment	T_{wall} (K)	T_{wall} (K)	$T_{interface}$ (K)	$T_{interface}$ (K)	$T_{interface}$ (K)	ΔT (K)
	Flownex®	RELAP5	Flownex®	RELAP5	Calculation Eq. (2-29)	Flownex®-Calculation
1	465.241	464.168	652.28	651.70	653.20	-0.93
2	465.153	464.166	652.19	651.70	653.20	-1.01
3	465.075	464.165	652.13	651.70	653.10	-0.97
4	465.052	464.164	652.11	651.70	653.10	-0.99
5	465.029	464.168	652.09	651.70	653.00	-0.91

4.3 Distributed heat sources

The next conduction analysis was performed on the nichrome wire, to which in the context of the SNUF experiments, an electric current was applied, thus generating an internal heat source. It was assumed that the power distribution was constant both radially and axially. The cylindrical geometry was modelled for both the RELAP5 and the Flownex® cases. In the RELAP5 case, the power was modelled as a distributed heat source and the results were compared with those predicted by Eq. (2-27). Eq. (2-27) was calculated in Excel and the result is also shown in Figure 4-5. The Flownex® and the RELAP5 interface temperatures of 648.96 K and 645.09 K respectively, showed good agreement with each other as can be seen in Table 4-13.

However, the temperature at the centre of the heat structures showed a marked difference. The Flownex® centreline temperature was observed to be 1186.10 K and the RELAP5 temperature was 837.56 K for two radial discretisations. It was observed that the Excel calculation temperature of 849.36 K was in good agreement with the RELAP5 centreline temperature. In Flownex®, the equation that was applied to solve the heat conduction was without volumetric sources, whereas in RELAP5, the equation which was used included volumetric sources. To compensate for this, the single nichrome heat structure was split into parallel slices in cylindrical geometry, with equal power sources placed at interfaces between the slices and at the surface at the extreme left with the total heat applied being conserved.

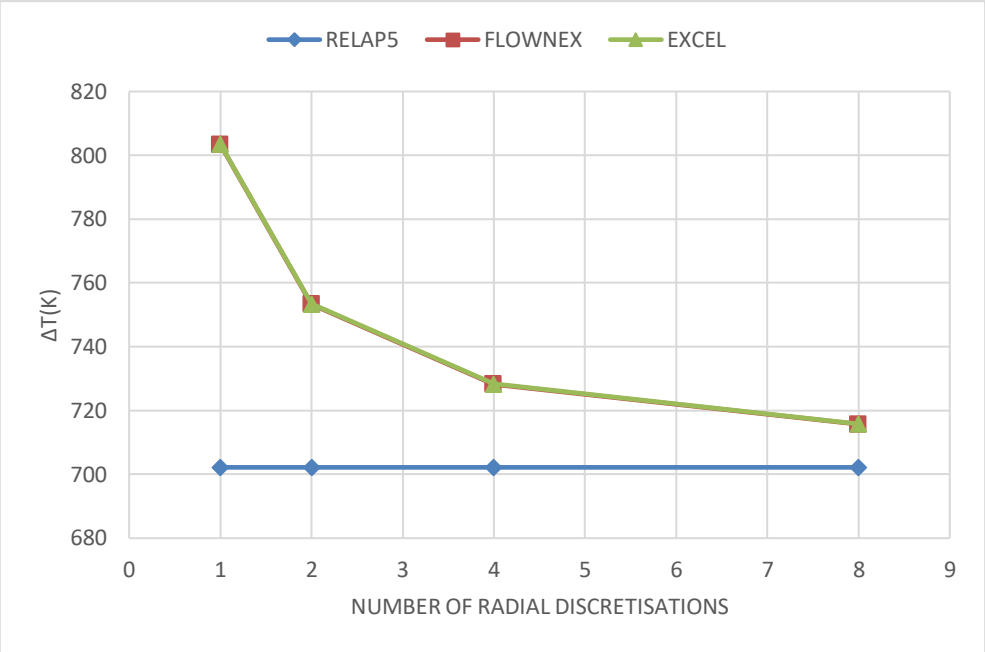

Figure 4-5: ΔT as a function of radial discretisations for the nichrome wire.

Table 4-13: Cylindrical geometry: radial discretisation.

	$T_{interface}$ (K)	$T_{interface}$ (K)	$T_{centreline}$ (K)	$T_{centreline}$ (K)	$T_{centreline}$ (K)	ΔT (K)
	Flownex®	**RELAP5**	**Flownex®**	**RELAP5**	**Calculation**	**Flownex®-Calculation**
2 Radial Discretisation	648.96	645.09	1186.10	837.56	849.36	336.74
4 Radial Discretisation	648.97	645.09	1036.38	837.56	849.36	187.02

Table 4-14: Cartesian geometry: discretisation of the nichrome wire

	$T_{interface}$	$T_{interface}$	$T_{centerline}$	$T_{centerline}$	$T_{centerline}$		ΔT
	FLOWNEX®	**RELAP**	**Flownex®**	**RELAP5**	**Calculation Eq. (2-35)**	**Eq. (2-36)**	**Flownex®-Calculation**
1 Radial discretisation	603.10	602.02	803.39	702.21	702.20	803.5	101.19

2 Radial discretisation	603.01	602.02	753.29	702.21	702.20	753.4	51.09
4 Radial discretisation	603.01	602.02	728.25	702.21	702.20	728.3	26.05
8 Radial discretisation	603.01	602.02	715.72	702.21	702.20	715.8	13.52

It was observed that as the number of the radial discretisations was increased, the temperature difference across the nichrome wire calculated, using the Flownex® package, approached that of the RELAP5 calculation as is shown in Figure 4 9. However, even with 8 discretisations modelled, the Flownex® centreline temperature was 715.72 K which was still not in agreement with the RELAP5, and the Excel calculated value of 702.21 K as shown in Table 4-14. The finding was that the distributed heat structure element provides more accurate temperature predictions than a heat source applied to the surface on one side of the conduction element.

4.4 Axial discretisation of the heated channel

In addition to the radial discretisation, as was discussed above, the axial discretisation of the fluid channel was also studied. The mass and energy conservation equations were solved using the axial discretisation of the core. This was done with the aid of Eqs. (2-1), (2-3) and (2-4). A constant axial power distribution was applied. Discretisation of 10 and 20 sub-units, in addition to the 5 units of the model with cylindrical geometry were carried out for the RELAP5 model. The results are presented in Table 4-15. The temperature as a function of axial height is plotted in Figure 4-6. With the difference in temperature at comparable axial positions being less than 0.1 K, it was considered that the core channel was adequately discretised using 5 units.

Table 4-15: RELAP5 cylindrical geometry with 5,10 and 20 axial discretisations

Discretisations	Channel Height (m)	Fluid Temperature (K)
5	0.24	424.95
5	0.48	427.204
5	0.72	429.466

5	0.96	431.721
5	1.2	434.196
5	0.24	424.95
10	0.12	423.829
10	0.24	424.943
10	0.36	426.07
10	0.48	427.202
10	0.6	428.334
10	0.72	429.467
10	0.84	430.597
10	0.96	431.726
10	1.08	432.847
10	1.2	434.195
20	0.06	423.281
20	0.12	423.827
20	0.18	424.381
20	0.24	424.94
20	0.3	425.503
20	0.36	426.068
20	0.42	426.634

20	0.48	427.201
20	0.54	427.768
20	0.6	428.334
20	0.66	428.901
20	0.72	429.467
20	0.78	430.033
20	0.84	430.598
20	0.9	431.162
20	0.96	431.726
20	1.02	432.289
20	1.08	432.852
20	1.14	433.409
20	1.2	434.195

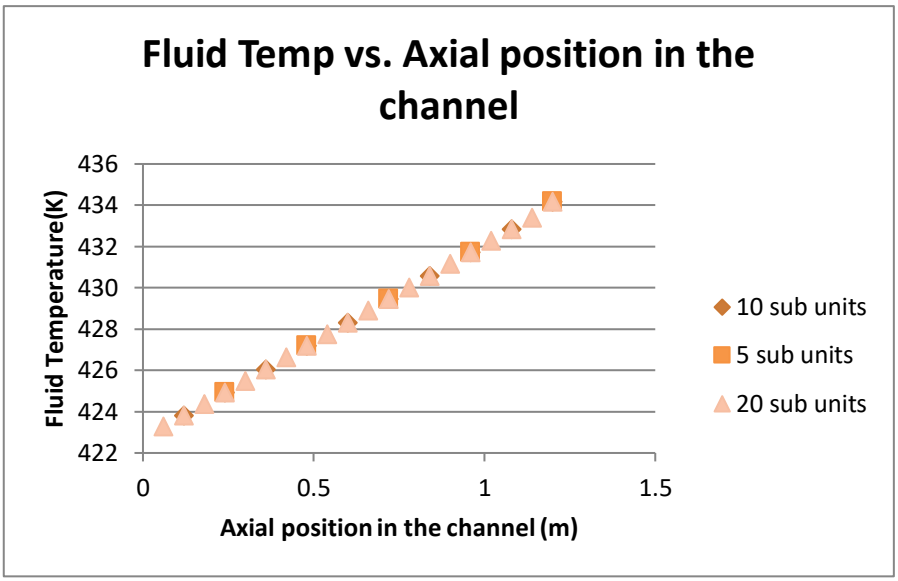

Figure 4-6: Axial discretisation of the heated channel.

4.5 Comparison of pressure drops between RELAP5 and Flownex®

This section of the study was based on the initial RELAP5 steady state model represented as a combination of six pipes modelled as a singular system of the core region. The core which formed an essential part of the study was divided into five increments. This model formed the basis for all models which were undertaken in this study. The input specifications required were the inlet mass flow rate, pressure, and temperature. The inlet pressure and initial cold and hot leg temperatures were listed in Table 3-1. RELAP5 calculations were performed, and the mass flow rate was adjusted to yield the required hot leg temperature. The mass flow rate for the RELAP5 model remained constant at 57.327 kg/s for the entire test period.

The pressure which was 15.7400 MPa at the time dependent volume (input boundary) had a steady decline all the way to 14.8107 MPa at the outlet volume. Flows in reactor systems are nearly always turbulent such that the Reynolds number is larger than 5000. The pressure drop observed in the results is partly due to the friction experienced in the pipes. Furthermore, the loss in pressure can also be attributed to the inlet and exit losses of the vessel, the local losses associated with the pipe bends as well as the crossflow losses in the pipes. The largest pressure drop of 0.57610 MPa was observed at pipe 170 which is an annulus, where secondary flow patterns may exist that increase the pressure losses in that flow section.

Since this was a steady state simulation the temperature remained constant throughout the system as expected. Other than the pipe parameters sourced from the MARS input file some values were calculated and are given in Table 4-17. The geometric and hydraulic circumferences are given in Table 4-17. The differentiating factor between the geometrical and hydraulic circumference is the geometrical diameter and the hydraulic diameter. If pipes are of a circular cross section, we use the conventional value for the diameter to find the Reynolds number, given by Eq. (2-32), when looking to verify whether the fluid flow in a pipe is laminar or turbulent. The geometrical circumference can then be found in the following manner:

$$C = \Pi D \tag{4-1}$$

where D is the geometrical diameter.

If the pipe has a non-circular cross section, a good approximation of the diameter can be found by using the equivalent diameter, otherwise known as the hydraulic diameter. This hydraulic diameter can be defined as:

$$De = 4 \times \frac{Free\ Flow\ Area}{Total\ wetted\ perimeter} \tag{4-2}$$

The hydraulic diameter then becomes the same as the actual diameter for a circular pipe. From the above equation, the circumference associated with the hydraulic diameter can be found, as it is the same as the total wetted perimeter, so the above equation then becomes:

$$C = \frac{(4 \times A)}{De} \tag{4-3}$$

The forward losses (A_F) given in Table 4-16 represent the Reynolds number independent forward flow energy loss coefficient. This quantity is used in each of the phasic momentum equations when the junction velocity of that phase is positive or zero (Information Systems Laboratories, 2001). Then, reverse losses (A_R) are the Reynolds number independent reverse flow energy loss coefficient. This quantity is used in each of the phasic momentum equations when the junction velocity of that phase is negative.

Table 4-16: Pipe parameters taken from the MARS output file.

Pipe	Direction	Flow Area [m^2]	Length [m]	Roughness [m]	Hydraulic Diameter [m]	A_F	A_R
110	90	0.049	1.200	2.000E-06	0.000	-	-
991	-90	0.003	0.145	4.572E-05	0.040	0	0
990	-90	0.003	0.120	4.572E-05	0.040	0	0
170	-90	0.003	0.153	4.572E-05	0.040	0	0
160	90	0.028	0.155	4.572E-05	0.190	3.93	3.93
180	90	0.071	0.153	4.572E-05	0.300	0	0
190	90	0.049	0.120	4.572E-05	0.021	0	0
195	90	0.049	0.120	4.572E-05	0.021	-	-
200	90	0.049	0.151	4.572E-05	0.021	0	0
210	90	0.049	0.120	4.572E-05	0.021	0	0

Table 4-17: Calculated pipe parameters.

Pipe	R [m]	D [m]	Flow Area [m^2]	L [m]	[2] HC [m]	[3]GC [m]	Elevation [m]	Roughness [m]
110	0.125	0.251	0.049	1.200	0.251	0.788	-1.616	2E-06
991	0.033	0.066	0.003	0.145	0.341	0.207	-0.416	4.572E-05
990	0.033	0.066	0.003	0.120	0.341	0.207	-0.561	4.572E-05
170	0.033	0.066	0.003	0.153	0.341	0.207	-0.681	4.572E-05
160	0.095	0.190	0.028	0.155	0.596	0.596	-0.834	4.572E-05
180	0.150	0.300	0.071	0.153	0.943	0.943	-0.679	4.572E-05
190	0.125	0.251	0.049	0.120	9.315	0.788	-0.530	4.572E-05
195	0.125	0.251	0.049	0.120	9.315	0.788	-0.410	4.572E-05
200	0.125	0.251	0.049	0.151	9.315	0.788	-0.290	4.572E-05

[2] Hydraulic circumference
[3] Geometric circumference

210	0.125	0.251	0.049	0.120	9.315	0.788	-0.139	4.572E-05

4.5.1 RELAP5 pressure drops

The pressure drops and mass flow rates as calculated in RELAP5 are shown in Table 4-18. The temperature changes are shown in Table 4-19. The negative mass flow sign for pipe 991 in Table 4-18 indicates that it acts as a mass flow inlet, linked to the time dependent volume. The pressure drop at the time dependent volume (pipe 110) was very large with a value of 0.266 Pa. More elaboration on this large pressure drop will follow in Section 4.5.2. The pressure drop from pipe 991 continued to decrease towards pipe 210 at the bottom. A significant divergence was observed at the annulus (pipe 170) with a pressure drop of 0.576 Pa. The temperature change at the time dependent volume (pipe 110) recorded the largest difference value with a ΔT of 0.095 °C as seen in Table 4-19. The temperature change across the other pipes was small and could be considered negligible.

Table 4-18: RELAP5 pressure drops and mass flows.

Pipe	Pi [MPa]	Po [MPa]	ΔP [MPa]	ṁ [kg/s]
110	15.740	15.474	0.266	57.327
991	15.474	15.462	0.012	-57.327
990	15.462	15.407	0.055	57.327
170	15.407	14.831	0.576	57.327
160	14.831	14.823	0.007	57.327
180	14.823	14.821	0.003	57.327
190	14.821	14.816	0.005	57.327
195	14.816	14.815	0.001	57.327
200	14.815	14.813	0.001	57.327
210	14.813	14.811	0.003	57.327

Table 4-19: RELAP5 temperature changes.

Pipe	Ti [°C]	To [°C]	ΔT [°C]
110	290.855	290.760	0.095
991	290.760	290.758	0.002
990	290.758	290.751	0.007
170	290.751	290.750	0.001
160	290.541	290.539	0.002
180	290.539	290.538	0.001
190	290.538	290.538	0.000
195	290.538	290.538	0.000
200	290.538	290.537	0.001
210	290.537	290.512	0.025

4.5.2 Flownex®

The Flownex® model, replicating the RELAP5 steady state model, had an input pressure of 15.7400 MPa similar to the RELAP5 boundary condition. However, a value of 15.4855 MPa was observed at the node downstream the boundary and upstream pipe 110. An outlet pressure of 14.8517 MPa was observed at pipe 210. There was also a significant loss in pressure, because of the friction losses, like the ones mentioned in the RELAP5 discussion above. Table 4-20 summarises the Flownex® results for the steady state model. The mass flow rate remained constant throughout the system at 57.327 kg/s. During flow through a fuel assembly, there will be pressure drop caused by friction forces on the surface, secondary losses and by gravity. The pressure losses mentioned were simulated in RELAP5. In Flownex®, in order to determine the correct pressure drop, the surface roughness of the material that is to be simulated, is specified according to the material specifications. The difference in the pressure drop values between the RELAP5 and the Flownex® results are also recorded in Table 4-20. The largest pressure drop value was observed at pipe 170. The largest deviation in pressure drop of the Flownex® model from the RELAP5 model was at pipe 110. The inlet and outlet temperatures from both models are consistent with each other from pipe 110 to pipe 210 as shown in Table 4-21.

The temperature was also observed to remain constant at approximately 290.855 °C The pressure drops were measured and compared from the outlet of the time dependent volume which is pipe 110. Measurements could not be taken at the inlet of the time dependent volume, as the results between the Flownex® and the RELAP5 models could not be compared accurately as the time dependent volume of RELAP5 applies a larger pressure drop than pipe 110 of the Flownex® model. The differences between the RELAP5 and the Flownex® pressure drops are indicated as a percentage change in Table 4-20Table 4-20 to further indicate the discrepancy between the pressure drops. This discrepancy would suggest that further studies still need to be carried out on the time dependent volume.

Table 4-20: Flownex® pressure drops, mass flows and delta errors between RELAP5 and Flownex®.

Pipe	Pi [MPa]	Po [MPa]	ΔP [MPa]	$\Delta P_R - \Delta P_F$ [MPa]	% Change	$\dot{m}$ [kg/s]
110	15.486	15.474	0.012	0.255	95.5	57.327
991	15.474	15.465	0.009	0.003	25	57.327
990	15.465	15.457	0.008	0.047	85.5	57.327
170	15.457	14.890	0.567	0.009	1.6	57.327
160	14.890	14.861	0.028	-0.021	-300	57.327
180	14.861	14.860	0.002	0.001	33.3	57.327
190	14.860	14.858	0.002	0.003	60	57.327
195	14.858	14.856	0.002	-0.001	-100	57.327
200	14.856	14.854	0.002	-0.001	-100	57.327
210	14.854	14.852	0.002	0.001	33.3	57.327

Table 4-21: Flownex® temperature changes.

Pipe	Ti [°C]	To [°C]	ΔT [°C]
110	290.855	290.852	0.003
991	290.852	290.853	-0.001
990	290.853	290.853	0.000
170	290.853	290.853	0.000

160	290.853	290.853	0.000
180	290.853	290.852	0.001
190	290.852	290.852	0.000
195	290.852	290.852	0.000
200	290.852	290.852	0.000
210	290.852	290.851	0.001

This section of the study was based on the initial RELAP5 steady state model of the core region which successfully formed the basis for all models which were undertaken in this study. The study on the heat transfer side indicated how the simulation models need to take nucleate boiling into account, so the pressure drop correlations can also be expected to be the same. As a result of this observation, future work can be to investigate the implementation of nucleate boiling pressure drop correlations in Flownex®, since the standard built in equations only provide for single phase liquids or homogeneous mixtures.

CHAPTER 5 CONCLUSIONS AND RECOMMENDATIONS

The following chapter gives the conclusions to the study. The recommendations for future studies and for the Flownex® simulation package are also given.

5.1 Conclusions

The Flownex® and the RELAP5 models of the core and downcomer section of the SNUF required for the comparisons of the thermo-hydraulic and heat transfer calculations were successfully built and run. The results from these simulations allowed for several conclusions to be drawn. When calculating the heat transfer coefficient, a conclusion was made that the Dittus-Boelter correlation in Flownex® produced unrealistic wall temperatures for the set of conditions used. Another conclusion was that the Chen correlation produced good agreement with the RELAP5 results. An observation was also made that there was a good correspondence between RELAP5 and Flownex® in the nucleate boiling region but not in the single-phase liquid region. A possible reason for this discrepancy could be within the implementation of the Dittus-Boelter correlation, so it is recommended that a laminar correlation be included in the C# script and a turbulent correlation be included in the Dittus-Boelter correlation for single-phase liquid and then tested in Flownex®.

When coming to the conduction analysis, it was concluded that discretisation of the component for both RELAP5 and Flownex® must be properly applied to get consistent results. The conduction element which required surface sources did not give satisfactory results, unless a large number of discretisations were used. Also, when the stainless-steel casing was included with the distributed heat source element, the results differed. An observation was made whereby the pressure drop values could not be analysed effectively at the inlet of the time dependent volume as the results between the Flownex® and the RELAP5 models could not be compared accurately because the time dependent volume in RELAP5 applied a larger pressure drop than pipe 110 in the Flownex® model. This discrepancy would suggest that further studies still need to be carried out on the use of the time dependent volume and the appropriate Flownex® equivalent component. Another key influencing factor to be noted in this study is that the pressure used during this study falls outside the range of the Chen correlation. To account for this, it is recommended that the calculated temperatures found in this study should be compared to

experimental values to validate the Chen correlation within this range. These experimental values were unfortunately unavailable for this validation process.

5.2 Recommendations

When calculating the heat transfer coefficient in Flownex®, it is suggested that the Chen correlation also be provided as a built-in correlation of Flownex®, rather than as a user coded script for nucleate boiling applications, as this is a labour intensive and time consuming process, that prevents automation of the Flownex simulation cycle. It is also recommended that future networks be built and compared with Flownex® and RELAP5 with more components of the thermo-hydraulic cycle of the SNUF.

REFERENCE LIST

Allison, C.M., Hohorst, J.K., & D'arcy A.J. 2009. Role of RELAP/SCDAPSIM in research reactor safety.Paper presented at RRFM 2009: Vienna March 2009.

ASME. 1967. Thermodynamic and transport properties of steam. 6th ed. New York: American Society of Mechanical Engineers.

Bergman, T.L., Lavine A.S., Incropera F.P., & Dewitt, D.P. 2011. Fundamentals of heat and mass transfer. 7th ed. John Wiley and Sons.

Bird, R.B., Stewart, W.E. & Lightfoot, E.N. 1960. Transport Properties. 2nd ed. New York: Wiley and Sons.

Britannica, E. 2019. Encyclopedia Britannica. [Online]
https://www.britannica.com/technology/computer-simulation
Date of access: 20 June 2019.

Bae, B-U., Park, C-H., Park, G-C., Suh, K-Y., & Lee, U-C. 2005. Thermal-hydraulic calculations using MARS code applied to low power and shutdown probabilistic safety assessment in a PWR. Seoul: Elsevier.

Byoung, U.B., Keo, H.L., Yong, S.K., Byong, J.Y., & Goon, C.P. 2008. Scaling methodology for a reduced-height reduced-pressure integral test facility to investigate direct vessel injection line break SBLOCA, 41(5):17. Seoul: Elsevier.

Center for International Governance Innovation. 2019. The IPCC report will have profound effects on climate governance. [Online]
https://www.cigionline.org/articles/ipcc-report-will-have-profound-effects-climate-governance?gclid=CjwKCAjwzJjrBRBvEiwA867byk-FntrugHlOBkB_N5A_t3TEkhYrNAbVntq0hwhlP7pm6aGCM7yPShoCuqoQAvD_BwE
Date of access: 2019.

Cengel, Y., Turner, R.H. and Cimbala, J.M. 2008. Fundamentals of thermal-fluid sciences. 3rd ed. McGraw-Hill.

Cilliers, C. 2012. Thermal-fluid simulation of nuclear steam generator performance using Flownex and RELAP5/mod3.4. Potchefstroom: PU for CHE. (Dissertation-MSc).

DoE. 2019. Integrated resource plan, Pretoria: Government gazette.

Eberhard, A. 2011. The future of South African coal: market, investment, and policy challenges.

www.flownex.com
Date of access: 2019.

F-chart. 2019. F-chart sftware.com. [Online]
http://fchartsoftware.com/ees/
Date of access: March 2019.

Flownex®. 2019. Flownex® theory manual. [Online]
www.flownex.com
Date of access: 2019.

Flownex®. 2020. Flownex® Simulation Environment. [Online]
https://www.flownex.com/client-faq/item/479-quality
Date of access: 8 April 2020.

Fourie, L. 2011. Thermal-hydraulics simulation of a benchmark case for a typical Materials Test Reactor using RELAP5 MOD4.0. Potchefstroom: PU for CHE. (Dissertation-MSc).

Glenn, A.R. & Fatih, A. 2014. Theory and implementation of nuclear safety system codes-Part 1: Conservation equations, flow regimes, numerics and significant assumptions. Idaho.

Incropera, F.P. & De Witt, D.P. 2002. Heat and mass transfer. 5th ed. John Wiley and Sons.

Information Systems Laboratories, I. 2001. RELAP5/MOD3.3 code manual volume 1. Washington DC: U.S. Nuclear Regulatory Commission.

KEPCO/KHNP. 2011. Status report 83 - Advanced Power Reactor 1400 MWe (APR1400).

Kim, Y-S., Bae, B-U., Park, C-H., Park, G-C., Suh, K-Y., & Lee, U-C. 2005. RELAP5/MOD3.3 analysis of coolant depletion tests after safety injection failure during a large-break loss-of-coolant accident. Seoul: Elsevier.

Lamarsh, R.L & Barrata, A.J. 1982. Introduction to nuclear engineering. 2nd ed. Addison-Wesley Publishing Company .

Leap. 2019. Leap Austrailia. [Online]
https://www.computationalfluiddynamics.com.au/convergence-and-mesh-independent-study/

Lee, K.H., Bae, B.U., Kim, Y.S., Chun, J.H. & Park, G.C. 2008. An experimental study with SNUF and validation of the MARS code for a DVI line break LOCA in the APR 1400, Seoul: Elsevier.

Leeb, N. 2016. M-Tech Industrial. Personal interview. Potchefstroom.

Mason, E.A. & Saxena, S.C. 1958. Approximate formula for the thermal conductivity of gas. The physics of fluid, 1: 361-369.

M-Tech. 2013. Flownex® simulation environment: general user manual. Potchefstroom.

M-Tech. 2015. Flownex® library manual. Potchefstroom.

NASA. 2008. NPARC alliance CFD verifcation and validation website. [Online]
https://www.grc.nasa.gov/www/wind/valid/tutorial/spatconv.html
Date of access: 28 June 2017.

Ragheb, M. 2011. Three Mile Island. 4 April.

RELAP5. 2010. RELAP5.MOD3.4 Code manual, Volume 1: code structure, system models, and solution methods. Nuclear Safety Analysis Division, Information Systems Laboratories, Inc., Idaho Falls, U.S.A.

RELAP5. 2010. RELAP5/MOD3.4 Code manual, Volume 4: Models and Correlations. Nuclear Safety Analysis Division, Information Systems Laboratories, Inc, Idaho Falls, U.S.A.

ResearchGate. 2020. ResearchGate. [Online]
https://www.researchgate.net/figure/Typical-boiling-curve-and-regimes-ONB-onset-of-nucleate-boiling-CHF-critical-heat-flux_fig6_268746847
Date of access: 21 November 2020.

Schmidt, E. 1 969. Properties of water and steam in SI units. 2nd ed. New York: Springer-Verlag.

Slabbert, R. 2011. Thermal-hydraulics simulation of a benchmark case for a typical Materials Test Reactor using Flownex, Potchefstroom: PU for CHE. (Dissertation-MSc).

Son, Y-S., Shin, J-Y., Lim, H-G., Park, J-H., and Jang, S-C. 2005. Thermal-hydraulic calculations using MARS code applied to low power and shutdown probabilistic safety assessment in a PWR. Seoul: Elsevier.

Stacey, W. 2007. Nuclear reactor physics. 2nd ed. Weinheim: Wiley.

Todreas, N.E. & Kazimi, M.S. 1990. Nuclear Systems 1, Thermal hydraulic fundamentals. Hemisphere Publishing Corporation.

Vegter, I. 2019. Daily Maverick. [Online]
https://www.dailymaverick.co.za/opinionista/2019-08-13-mantashe-is-right-south-africa-must-build-more-nuclear-energy/

Date of access: 13 August 2019

Wilke, C.R. 1950. A viscosity equation for gas mixtures. J. Chem Physics, 18: 517-519.